DOTTORATO IN MEDICINA SPERIMENTALE

Curriculum Biochimica

XXX ciclo

settore scientifico disciplinare BIO/10

Abscisic acid: a promising molecule in the treatment of type 2 diabetes mellitus and its complications

Supervisor

Elena Zocchi

Santina Bruzzone

PhD thesis

Valeria Booz

Anno Accademico 2017

INDEX

ACKNOWLEDGEMENTS

This study, with the title “Abscisic acid: a promising molecule in the treatment of type 2 diabetes mellitus and its complications”, is an experimental project carried out in the period from November 2014 to October 2017 at the Department of Experimental Medicine (DIMES), section of Biochemistry, University of Genova, School of Medicine under the supervision of Professor Elena Zocchi and Santina Bruzzone.

I would like to say thanks to Elena Zocchi for her engagement in the project and for making the study a possibility at all. Thanks to Santina Bruzzone for teaching me the practical terms of experiment setting, and for always having the patience and time to answer my questions. Thanks to Giovanna Sociali and Tiziana Vigliarolo for supporting me for all the PhD period.

I spent 5 months at the Department of Biomedical Sciences, University of Copenhagen under the supervision of Professor Holst Jens Juul, and I wish to thank Prof. Holst and the PhDs Charlotte Bayer Christiansen, Monika Saltiel and Rune Kuhre for their support in conducting the experiments using the perfusion models, allowing me to obtain the results presented in this thesis.

Valeria Booz

LIST OF ABBREVIATIONS

ABA: Abscisic acid

AC: Adenylyl cyclase

AKT: Protein kinase B

APD: Adenosine diphosphate ribose

AP2: Adipocyte protein 2

ATMSC: Human mesenchymal stem cells

AT: Adipose tissue

BAT: Brown adipose tissue

cAMP: 3'5'-cyclic adenosine monophosphate

cADPR: Calcium mobilizer cyclic ADP-ribose

CD38: Cluster of differentiation 38

CIDE-A: Cell death activator CIDE-A

DPP-IV: Dipeptidyl peptidase 4

ERK: Extracellular signal-regulated kinase

GAPDH: Glyceraldeyde-3-phosphate dehydrogenase

GLP-1: Glucagon-like peptide 1

GLUT-4: Glucose transporter 4

GMD: Gestational diabetes mellitus

IVGTT: Intravenous glucose tolerance test

LANCL2: lanthionine synthetase component C-like-2

L-NAME: NG-nitro-L-arginine methyl ester

MAPK: Mitogen-activated protein kinase

MCP-1: Monocyte chemoattractant protein-1

mTORC2 : Mechanistic target of rapamycin Complex 2

NO: Nitric oxide

NOS: Nitric oxide synthase

OGTT: Oral Glucose Tolerance Test

PGC-1α: Peroxisome proliferator-activated receptor gamma coactivator 1-alpha

PI3K: Phosphoinositide 3-kinase

PKA: Protein kinase A

PPAR: Peroxisome proliferator-activated receptors

PRDM16: PR domain containing 16

PTX: Pertussis toxin

TDCA: Taurodeoxycholate

T1DM: Type 1 diabetes mellitus

T2DM: Type 2 diabetes mellitus

TMEM26: Transmembrane protein 26

TNFα: Tumor necrosis alpha

TZDs: Thiazolidinediones

UCP-1: Mitochondrial uncoupling proteins 1

WAT: White adipose tissue

SUMMARY

Type 2 diabetes mellitus (T2DM) is a chronic metabolic disorder characterized by high blood sugar, insulin resistance, and relative insulin insufficiency. Being a life-long condition, T2DM exposes affected subjects to life-threatening sequelae, which typically arise one or more decades after disease onset, consisting of cardiovascular disease, stroke, and diabetic neuropathy, all sustained by the widespread damage to the microcirculation, caused by the metabolic derangement.

The number of T2DM patients by 2035 is projected to reach 592 million people worldwide, rising concern among the National Health Care Institutions regarding the sustainability of health care to the increasing T2DM population. For this reason, a concerted effort is underway within the scientific community to meet the demand for innovative therapeutic and preventive strategies for T2DM treatment. While T2DM is a life-long condition, pre-diabetes is reversible: thus, pharmacological and life-style interventions aimed at preventing or delaying the progression of pre-diabetes to the overt disease are currently investigated.

Interestingly, the plant hormone abscisic acid (ABA) has been recently identified as a new mammalian hormone involved in the regulation of glycaemia through its receptor LANCL2, paving the way to the potential use of ABA as a new therapeutic in diabetes. Among the currently utilized anti-diabetic drugs, GLP-1 mimetics reduce glycemia and also provide neuro- and cardio-protective effects, which are particularly advantageous in the diabetic patient.

The aims of my thesis were the following: i) to investigate the functional cross-talk between GLP-1 and ABA *in vitro* and *in vivo* on a rodent whole-body perfusion model, and to investigate the possible neuroprotective role of ABA (I chapter); ii) to

investigate the role of the ABA/LANCL2 system in the regulation of glucose uptake, adipogenesis and adipocyte browning in rodent and human adipocytes (II chapter).

Parts of the results described in the 1st and 2nd chapter of this thesis have been already published (Bruzzone S et al, Plos One 2015 and Sturla L et al, Biochim Biophys Acta 2017). I performed all the experiments described in this thesis.

[Bruzzone S, Magnone M, Mannino E, Sociali G, Sturla L, Fresia C, **Booz V**, Emionite L, De Flora A, Zocchi E. Abscisic Acid Stimulates Glucagon-Like Peptide-1 Secretion from L-Cells and Its Oral Administration Increases Plasma Glucagon-Like Peptide-1 Levels in Rats. PLoS One. 2015].

[Sturla L, Mannino E, Scarfì S, Bruzzone S, Magnone M, Sociali G, **Booz V**, Guida L, Vigliarolo T, Fresia C, Emionite L, Buschiazzo A, Marini C, Sambuceti G, De Flora A, Zocchi E. "Abscisic acid enhances glucose disposal and induces brown fat activity in adipocytes in vitro and in vivo." Biochim Biophys Acta. 2017].

I CHAPTER

1.0 Introduction

1.1. Abscisic acid

ABA is a phytohormone regulating several physiological responses in plants, such as seed dormancy, seedling development and tolerance to abiotic stress, including drought. ABA is an isoprenoid hormone (Fig. 1) and the naturally occurring enantiomeric form of ABA is (S)-ABA. The presence of ABA in animal tissues has been known since the 1980s [Le Page-Degivry et al, 1986]. Interestingly, in the last 10 years it has been demonstrated that ABA is present also in humans. Despite the kingdom-specific signaling and biosynthesis, there are also commonalities between plants and animals where both plants and animals rely on intracellular free ABA for activation of their receptors [Klingler et al, 2010].

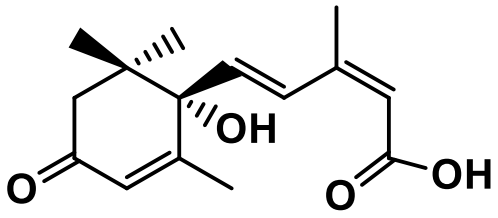

Fig. 1. Chemical structures of ABA

In the animal kingdom, several cell types produce and respond to ABA : innate immune cells (granulocytes, microglia, monocytes and macrophages), in which ABA functions as a novel inflammatory cytokine [Bruzzone S et al, 2007] ; mesenchymal and hematopoietic stem cells, which are expanded by ABA *via* autocrine and

paracrine mechanisms [Scarfi S et al, 2009]; β- pancreatic cells, in which ABA induces synthesis and release of insulin (both glucose-independent and glucose-stimulated) [Bruzzone S et al, 2008]; skeletal muscle cells and adipocytes, which respond to ABA with increased glucose uptake due to GLUT4 translocation on the plasma membrane [Bruzzone S et al, 2012 (a]. The multiplicity of functional effects exerted by ABA in animal cells suggests that endogenous ABA dysfunction may play a role in numerous diseases, including diabetes, metabolic syndrome, inflammatory and autoimmune diseases, atherosclerosis, and also that administration of exogenous ABA through nutritional sources or as a drug might have therapeutic potential.

1.2. The ABA signalling pathway

ABA regulates cell growth, development and immune responses to various stimuli through a signalling pathway that is similar in plants and mammals. It has been demonstrated that lanthionine synthetase component C-like-2 (LANCL-2) is an ABA receptor. LANCL-2 is a member of the highly conserved and widely distributed lanthionine synthetase component C-like (LANCL) protein family. LANCL-2 is associated with the plasma membrane through N-terminal myristolation [Landlinger C et al, 2006], and it is coupled to a G-protein responsible for the activation of the ensuing signalling cascade. Indeed, following ABA-binding to LANCL-2, adenylyl cyclase (AC) is activated, with generation of cyclic AMP, PKA (protein kinase A) stimulation, activation of the ADP-ribosyl cyclase CD38, overproduction of the universal calcium mobilizer cyclic ADP-ribose (cADPR) and increase of the intracellular calcium concentration ($[Ca^{2+}]_i$); this signalling cascade has been demonstrated in granulocytes, monocytes and insulin-releasing cells [Bruzzone et al, 2007 and 2008; Magnone M et al, 2009]. The G-protein coupled to LANCL-2 was identified as Gi by its sensitivity to pertussis toxin (PTX) [Bruzzone S et al, 2007], and it has been

demonstrated that the βγ subunits of Gi are responsible for the activation of AC [Sturla L et al, 2009]. The signalling pathway activated by LANCL2 is shown in Fig. 2. Upon ABA-binding, LANCL2 also translocates into the nucleus [Fresia C et al, 2016]. Thus, LANCL-2 combines features typical of peptide as well as of steroid receptors, making it an unprecedented example among the hormone receptors family. (Fig. 2)

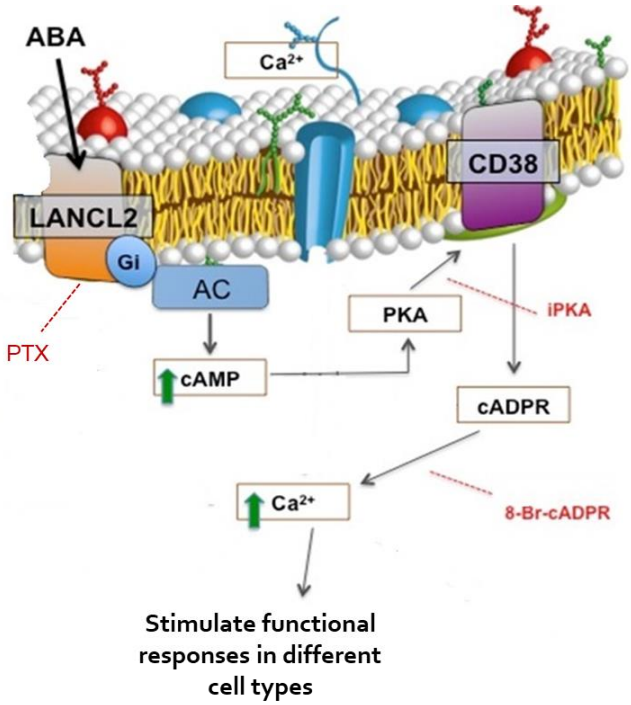

Fig. 2. The ABA signalling pathway.

1.3. Type 2 diabetes mellitus

Diabetes mellitus comprises type 1 diabetes (T1DM) and type 2 diabetes (T2DM). T1D is characterized by absolute insulin deficiency, whereas insulin resistance characterizes T2DM. T1DM is caused by the autoimmune destruction of pancreatic insulin-producing β-cells, while T2DM is caused by relative insulin deficiency due to insulin resistance. T2DM is indeed a complex chronic endocrine and metabolic disorder and the number of people with T2DM is significantly increasing in developing as well as in rich countries. It is estimated that in 2030 439 million people will be affected by T2DM [Chamnan P et al, 2011], with the principal risk factors depending on genetic predisposition–sedentary lifestyle, hypercaloric diet and consequent obesity [Kielgast U et al, 2009; Knop FK et al, 2009].

Pancreatic insulin and glucagon are the primary regulators of blood glucose levels. Insulin is produced in β-cells and glucagon in α-cells, all arranged in the endocrine islets of Langerhans [Cabrera O et al, 2006]. Insulin signals that blood glucose is higher than necessary, stimulating cells to take up excess glucose for storage and to convert it into glycogen (liver and muscle tissue) or triacylglycerols (adipose tissue) [Saltiel AR et al, 2001]. Glucagon signals that blood glucose is too low, stimulating hepatic glucose production through glycogenolysis and gluconeogenesis [Gromada J et al, 2007]. When glucose enters the systemic circulation, insulin secretion is increased and glucagon secretion is decreased.

The pathophysiology of T2DM is caused by both β-cell dysfunction and insulin resistance. The β-cells are still capable of producing insulin but do not respond appropriately to elevated blood glucose causing relative insulin deficiency. Target tissues have a decreased insulin sensitivity and thus become “insulin resistant”, this term denoting a condition where excess insulin is required to achieve glycemic control. The decline in β-cell function of T2DM patients is attributed to chronic

hyperglycaemia, chronic exposure to non-esterified fatty acids, oxidative stress, inflammation, and amyloid formation. Patients with T2DM also have a pancreatic α-cell dysfunction that results in increased (or not suppressed) glucagon secretion in the presence of hyperglycaemia [Sakurai H et al, 1974; Holst JJ et al, 2008] and probably a reduced post-prandial GLP- 1 secretion. [Olokaba AB et al, 2012].

Glucagon-like peptide 1 (GLP-1) is an incretin hormone, produced by the intestinal epithelial endocrine L-cells. GLP-1 is derived from proglucagon, and proteolytic cleavage of the first six residues results in the biologically active peptide, GLP-1 (7–36) amide. GLP-1 is secreted in the bloodstream in response to nutrient intake, especially in response to meals high in fats and carbohydrates [Baggio LL et al, 2007], and is rapidly inactivated by the circulating peptidase DPP-IV (dipeptidyl peptidase 4) *in vivo*. One of the actions of GLP-1 is to stimulate insulin release from beta cells.

1.4. ABA in glycemia control

In the past 10 years several studies were performed, both *in vitro* and *in vivo*, to evaluate the possible use of ABA in the treatment of T2DM. Starting from the fact that the second messengers involved in ABA signalling, cAMP and cADPR, are known to play a role in the signalling pathway leading to glucose-induced insulin secretion and that acute physical stress induces hyperglycemia, a condition which leads to increased plasma ABA levels [Bruzzone S el al, 2012 (a], it was hypothesized that ABA might be involved in glycemia homeostasis and possibly in its dysregulation as well.

Indeed, ABA potentiates glucose-induced insulin release and stimulates glucose-independent insulin secretion from insulinoma cells and from murine and human β pancreatic islets. Furthermore, in these cell types, ABA activated the same signalling pathway shown in Fig. 2. These results were the first demonstration that ABA is an

endogenous stimulator of insulin secretion in human and murine pancreatic cells. [Bruzzone S et al,2008].

Furthermore, a study conducted by Guri AJ [Guri AJ at el, 2008] provided the first evidence *in vivo* that dietary ABA intake improves glucose tolerance in obese db/db (leptin receptor-deficient) mice fed a high fat diet. Indeed, ABA was shown to have a similar efficacy as thiazolidinediones (TZDs), and to increase the expression of PPAR γ in a mouse model of diet-induced diabetes [Guri AJ et al, 2008].

Beside stimulating insulin release from pancreatic β- cells, ABA exerts other effects impacting on glucose homeostasis. *In vitro* experiments with murine adipocytes and rat myoblasts demonstrated that nanomolar ABA stimulates glucose uptake *via* an increased translocation of the glucose transporter 4 (GLUT-4) to the plasmamembrane [Bruzzone S el al, 2012 (a]. Moreover, Bruzzone showed that plasma ABA (ABAp) increases after oral glucose load (OGTT) in normal subjects, and found a positive correlation between the ABA area under the curve (AUC) and the glucose AUC [Bruzzone S et al, 2012 (a]. The increase of ABAp in response to hyperglycemia is impaired in subjects with T2DM and in women with gestational diabetes (GDM) [Ameri P et al, 2015]. GDM is a glucose intolerance with onset during pregnancy and, unlike T2DM, it is a reversible condition. Indeed, restoration of normal glucose tolerance after childbirth was accompanied by normalization of the ABAp response to hyperglycemia [Ameri P et al, 2015]. GMD and T2DM subjects have in common the impairment of the response of ABAp to hyperglycemia compared with normal glucose-tolerant controls, suggesting a causal role of defective endogenous ABA in glucose intolerance.

Finally, an *in vivo* study has demonstrated that microgram amounts of ABA improve glucose tolerance without increasing insulinemia in rats and in healthy humans undergoing an OGTT compared with the untreated controls [Magnone M et al, 2015].

Altogether, these results indicate that ABA has a beneficial effect on glycemic control and that a dysfunctional endogenous ABA response to hyperglycemia occurs in diabetes mellitus.

Interestingly, little or no increase of ABAp was observed in healthy subjects, when glucose was administered intravenously (IVGTT) instead of orally, suggesting a role for incretins in stimulating endogenous ABA release [Bruzzone S et al, 2012 (a].

1.5. ABA and GLP-1 may be functionally intertwined

The latest therapeutic strategies for the treatment of TD2M are based on incretins, either with drugs mimicking the effects of GLP-1 (GLP-1 mimetics) or with drugs preventing the hydrolysis of circulating endogenous GLP-1.

The main actions of GLP-1 are to stimulate insulin secretion, to inhibit glucagon secretion, to delay gastric emptying, and to signal satiety in the central nervous system, thereby contributing to the reduction of postprandial glucose excursions. In T2DM, the loss of the incretin effect mainly reflects a reduced GLP-1 potency and an impaired secretion of GLP-1: pre-prandial administration of GLP-1 reduces plasma glucose and improves glucose tolerance [Todd JF et al, 1997].

In contrast to other insulinotropic agents, the insulinotropic effect of GLP-1 depends on hyperglycemia, allowing blood glucose normalization without the risk of hypoglycemia [Nauck MA et al, 1993]. However, due to its short circulating half-life, native GLP-1 is ill-suited for chronic therapy [Baggio LL et al, 2007]. The short half-life (1–2 min in humans) results from DPP4-mediated proteolysis, which rapidly removes the N-terminal dipeptide, inactivating GLP-1. A single GLP-1 dose, therefore, results in only a limited, short-lasting increase in insulin secretion and a correspondingly brief effect on the plasma glucose concentration [Holst JJ et al, 2009]. Two strategies have been developed to address this problem in the treatment of T2DM: 1) treatment with

synthetic GLP-1 receptor agonists that are resistant to degradation by DPP4 ("incretin mimetics") or 2) protection of endogenous GLP-1 (and GIP) by inhibition of DPP4, whereby the effect of GLP-1 will be prolonged (DPP4 inhibitors – "incretin enhancers") [Knop FK et al, 2009; Holst JJ et al, 2009].

Two lines of evidence suggest a functional cross-talk between endogenous ABA and GLP-1: i) as mentioned above, ABAp increases in healthy subjects after on oral, but not after an intravenous glucose load, which does not induce release of endogenous GLP-1 [Bruzzone S et al,2012 (a]; ii) GLP-1 stimulates ABA release from rat insulinoma cells and from human pancreatic islets, by ∼10- and 2-fold in low and high glucose, respectively [Bruzzone S et al, 2012 (a].

1.6. Diabetes and cerebrovascular disease

In the past 20 years, a dramatic increase in the prevalence of T2DM is being observed, which has been attributed to the increase in the prevalence of obesity. T2DM causes extensive microvascular and macrovascular damage, often resulting in cerebrovascular complications, including stroke and cognitive impairment. Moreover, diabetic neuropathy is a complication of diabetes that may affect the nervous system. This pathological condition results in part from the microangiopathy, and in part from the direct effect of hyperglycemia on neurons [Katona I et al, 2017].

Indeed, the prevalence of Alzheimer's disease and of vascular dementia is also on the rise, and T2DM is an established risk factor for both conditions [Riederer P et al, 2017].

1.7. eNOS and nitric oxide

Nitric oxide (NO) acts as a neurotransmitter and is involved in a variety of physiological processes in the brain, such as control of cerebral blood flow, interneuronal communications, synaptic plasticity, memory formation, receptor functions, intracellular signal transmission. NO is synthesized from L-arginine by nitric oxide synthase (NOS). Cerebral blood flow needs to be strictly regulated because the cerebral circulation supplies oxygen to the brain tissue and neuronal activation requires large amounts of metabolic energy [Moncada S et al, 1991].

Three isoform of NOS are present in the human body: endothelial nitric oxide synthase (eNOS), neuronal nitric oxide synthase (nNOS) and inducible nitric oxide synthase (iNOS) [Toda N et al, 2009]. eNOS is expressed in the vascular endothelium and choroid plexus. NO derived from eNOS plays a key role in preserving and maintaining the brain's microcirculation [Toda N et al, 2009].

Interestingly, ABA has been shown to stimulate NO production in different cell types, including the microglia, human granulocytes and keratinocytes [Bruzzone S et al, 2012 (b and 2007; Bodrato N et al, 2009].

1.8. ABA in the brain

In 1986, Le Page-Degivry [Le Page-Degivry et al, 1986] published the first evidence that ABA is present in the mammalian brain. This observation was obtained by using a very specific radioimmunoassay in brains of pigs and rats.

Thirty years later, Sanchez-Sarasua [Sanchez-Sarasua et al, 2016] showed that ABA can cross the blood brain barrier, that it has a protective effect against neuroinflammation caused by a high fat diet and that it restores cognitive function.

Chronic treatment with ABA in rats showed a beneficial antidepressant effect, which was attributed to the molecular structural similarities between ABA and retinoic acid [Qi CC et al, 2014].

Presence of ABA in the brain, together with the observation that the hormone can stimulate NO synthesis in innate immune cells, including microglia, suggests a possible role of ABA as an endogenous stimulator of NO production in the brain.

2.0 Aims of this study

In the past 10 years, ABA has been demonstrated to be involved in the regulation of glycemia in mammals. Indeed, ABA is released by human and murine pancreatic β-cells, an oral glucose load increases plasma ABA in healthy human subjects, ABA stimulates glucose uptake by rodent adipocytes and myoblasts and oral ABA intake improves glucose tolerance in rodents and in healthy humans. Moreover, GLP-1 stimulates ABA release from an insulinoma cell line and from human islets and indirect evidence points to the possible stimulation of ABA release by incretins in vivo in humans.

One aim of this study was to investigate the possible cross-talk between ABA and GLP-1, to elucidate a possible role of ABA in mediating the functional effects currently ascribed to GLP-1.

In particular, the first objective of this thesis was to investigate whether ABA affects GLP-1 secretion *in* vitro, using enteroendrocrine cells, and *in vivo*, on rodents.

Another aim of this study was to investigate the effect of ABA on the release of insulin and of GLP-1 in a perfused organ system, which allows to directly apply ABA to the target cells *in vivo*, via the circulatory system.

Finally, based on the observation that ABA induces NO release from microglia, we hypothesized a neuroprotective role for ABA, *via* stimulation of NO production. Dysregulation of ABA function in T2DM might thus be responsible for both the impaired glucose tolerance (*via* reduced insulin and GLP-1 release) and the increased risk of neurological damage (*via* the impairment of neuroprotective NO generation).

A third aim of my thesis was to investigate the effect of ABA on NO production and cell survival to hypoxia in the neuroblastoma cell line N2a as a model of neuronal cell.

3.0 Materials and Methods

3.1. *In vitro* and *in vivo* effects of ABA on GLP-1 release from L-cells

3.1.1. hNCI-H716 cell culture and GLP-1 secretion studies

The human L cell line hNCI-H716, derived from a poorly differentiated adenocarcinoma of the cecum, was obtained from the American Type Culture Collection (Manassas, VA). Cells were grown in suspension in RPMI-1640 (Sigma, Milano, Italy), supplemented with 10% fetal bovine serum (FBS), 50 U/ml penicillin and 50 µg/ml streptomycin.

For GLP-1 secretion assays, a protocol similar to the one described in [Reimer RA et al, 2001] was followed: briefly, hNCI-H716 cells were seeded on Matrigel matrix (Becton Dickinson, Bedford, MA), at the density of $2x10^5$cells/well in 24-well plates, in DMEM medium supplemented with 10% FCS, 50 U/ml penicillin, and 50 µg/ml streptomycin. After 48 h, cells were washed in Hank's Balanced Salt Solution (HBSS) and then incubated for 2 h in Krebs Ringer Hepes buffer (KRH buffer: 130 mM NaCl, 5 mM KCl, 1.3 mM $CaCl_2$, 25 mM HEPES, 10 mM Na_2HPO_4, 1.3 mM $MgSO_4$, 0.2% BSA), in the presence or absence of the different treatments: glucose (200 mM), or glutamine (10 mM), or ABA (0.1, 10 or 200 µM).

After treatment, medium and cells were collected separately: GLP-1 content in the supernatant was analyzed by GLP-1 Total ELISA Kit (Merck Millipore, Vimodrone, MI, Italy); total protein content in cells was analyzed by Bradford assay (Bio-Rad, Milano, Italy).

3.1.2. Quantitative real time-PCR

Total mRNA was extracted from hNCI-H716 using Qiazol (Qiagen, Milan, Italy) according to the manufacturer's instructions. Quality and quantity of RNA were analysed using a NanoDrop spectrophotometer (Nanodrop Technologies, Wilmington, DE). The cDNA was synthesized by the iScriptTM cDNA Synthesis Kit (Bio-Rad, Milan, Italy) starting from 1 µg of total RNA. PCR primers were designed through Beacon Designer 2.0 Software and their sequences were as indicated in Table 1.

Table 1. Primers

Human gene		Sequence, 5'-3'
GLP-1	Forward	GCTGAAGGGACCTTTACCAGT
	Reverse	CCTTTCACCAGCCAAGCATG
GLUCAGON	Forward	ATTCACAGGGCACATTCACCA
	Reverse	GGTATTCATCAACCACTGCAC
ACTIN	Forward	GCGAGAAGATGACCCAGATC
	Reverse	GGATAGCACAGCCTGGATAG
HPRT-1	Forward	GGTCAGGCAGTATAATCCAAAG
	Reverse	TTCATTATAGTCAAGGGCATATCC

qPCR was performed in an iQ5 real-time PCR detection system (Bio-Rad) using 2× iQ Custom Sybr Green Supermix (Bio-Rad). Values were normalized on mRNA expression of human β-actin and HPRT. Statistical analysis of the qPCR was performed using the iQ5 Optical System Software version 1.0 (Bio-Rad) based on the $^{2-}\Delta\Delta$Ct method [Sturla L et al, 2009]. The dissociation curve for each amplification was analysed to confirm absence of unspecific PCR products. Experiments were repeated three times in triplicate.

3.1.3. Measurement of the intracellular cAMP concentration

hNCI-H716 cells were seeded at the density of $5x10^5$/well in 12-well, Matrigel matrix-coated plates. After 24 h, cells were washed with HBSS, pre-incubated for 10 min in HBSS containing 10 µM IBMX, an inhibitor of phosphodiesterases, and then stimulated with 10 mM glutamine or 200 µM ABA for 2.5 and 5 min.

The supernatant was removed and cells were lysed in 0.6 M PCA. Intracellular cAMP content was evaluated by EIA (Cayman, Ann Arbor, MI, USA) on neutralized extracts [Moreschi I et al, 2006].

3.1.4 Vector construction

The full length LANCL2 cDNA was amplified by PCR using cDNA obtained with reverse transcription of total RNA from human granulocytes and using the following primers: 5'-CACCATGGGCGAGACCATGTCAAAG-AG-3'(forward);

5'ATCCCTCTTCGAAGAGTCAAGTTC-3'(reverse).

The PCR was performed in 25 µl containing undiluted reaction buffer, 200 µM dNTP, 5 pmol of primers and using 1.25 U of Herculase HotStart DNA polymerase. The PCR reaction profile was 1 cycle at 94°C for 2 min, 35 cycles at 94°C for 15 s, 62°C for 30 s and 72°C for 1 min with a final extension for 5 min at 72°C. The PCR product was purified with Nucleospin® Extract Kit (Macherey-Nagel) and cloned into pcDNA3.1/V5-His-TOPO©. This vector allows the synthesis of the recombinant protein as a C-terminal fusion to the V5 epitope and a Histidine tag. The LANCL2 plasmid was purified using PureLink™ HiPure Plasmid Filter Kit (Invitrogen) and sequenced by TibMolbiol (Genova, Italy).

3.1.5. LANCL2 overexpression

hNCI-H716 cells were transfected in parallel with pcDNA3.1(+) (control plasmid) or with the plasmid containing the full-length LANCL2 cDNA, LANCL2-pcDNA3.1(+) (LANCL2 plasmid). Transient transfection of hNCI-H716 cells ($1.5x10^6$) was performed using the Nucleofector System (Amaxa GmbH, Köln, Germany), program X-005, solution T, with 3 µg LANCL2-plasmid or control plasmid. hNCI-H716 cells were then resuspended in DMEM and seeded in Matrigel-coated 24-well plates. Experiments were performed 48 h after transfection.

3.1.6. Western blot analysis

hNCI-H716 cells ($2.5x10^5$) were lysed in 50 µl HES lysis buffer (20 mM Hepes, pH 7.4, 1 mM EDTA, 250 mM sucrose) containing a protease inhibitor cocktail (Sigma), and LANCL2 expression was analyzed by Western blot, using a monoclonal antibody against LANCL2 [Vigliarolo T et al, 2015]. LANCL2 expression was normalized on vinculin levels, detected with a goat polyclonal antibody against actin (Santa Cruz Biotechnology, Dallas, TX).

After SDS-PAGE, performed according to the standard method on 10% gels, proteins were transferred to a nitrocellulose membrane (Bio-Rad Laboratories). The membrane was blocked for 1 h with PBS-0.1% Tween 20 (PBST) containing 5% non-fat dry milk and incubated overnight at room temperature with the primary antibody. After washing with PBST, the membrane was incubated with an appropriate HRP-conjugated secondary antibodies (Cell Signaling, Danvers, MA; Santa Cruz Biotechnology) and developed with Immobilon™ Western Chemiluminescent HRP Substrate (Millipore, Milano, Italy), following the manufacturer's instructions. Band intensity was evaluated with the Chemidoc system (Bio-Rad Laboratories).

3.1.7. *In vivo* experiments

Two-months old female Wistar rats weighing 160 to 198 g (obtained from Charles River Laboratories Italia, Calco, LC, Italy) were housed singly under a 12 h/12 h light/dark cycle under free feeding conditions, in temperature- and humidity-controlled rooms.

After an overnight fast, the DPP4 inhibitor Sitagliptin (Januvia®, 10 mg/Kg) [Forest T et al, 2014], was orally administered 30 min prior to ABA (50 mg/Kg) or vehicle (water) gavage. After anesthesia with ketamine/xylazine, blood samples were collected at 0, 20, 40 and 60 min by orbital sinus bleeding in heparin and plasma aliquots were stored at -20°C. The dose of ABA was chosen based on the effect of dietary ABA supplementation [Guri AJ et al, 2007].

In other experiments, where animals were not pre-treated with Sitagliptin, GLP-1 concentration was also evaluated in the portal vein blood, as in [Hirasawa A et al, 2005], 10 min after intragastric vehicle or ABA administration.

Animal rearing conditions were consistent with the guidelines of the Italian Ministry of Health and the study was approved by the IRCCS AOU San Martino-IST Ethical Committee (Genova, Italy).

3.1.8. Measurements of plasma GLP-1, glucose, insulin and ABA

Plasma GLP-1 concentrations were determined by ELISA (Merck Millipore; the kit detects the total GLP-1 levels). Glycemia was measured with a glucometer (Bayer, Milano, Italy) and insulinemia by ELISA (Bertin-Pharma, Montigny, France). ABA plasma concentrations were determined by ELISA, with a sensitive and specific kit (Agdia), according to the manufacturer's instructions and measuring absorption at 405 nm [Bruzzone S et al, 2012 (a].

3.2. Insulin, GLP-1 and ABA release from rat pancreas and proximal small intestine

The perfused-organ setting allows to better explore the physiology of hormone secretion compared to the *in vitro* experimentation on isolated cells.

The perfused pancreas and intestine maintains a correct cell polarity and correct cellular functional capacity and vascular/neuronal integrity as opposed to isolated cell cultures. In the perfused organ, maintenance of the cytoarchitecture and the vasculature allows for the study of metabolic, endocrine and paracrine factors.

Isolated islets of Langerhans from rats mainly reflect metabolism of the insulin-producing β cells since they constitute the major part of the islets. Furthermore, the islets lose their natural orientation concerning cytoarchitecture and vasculature when isolated. Important to note is also that the secretion using this model occurs by diffusion, which is not the mechanism by which the products are secreted *in vivo* [Samols E et al,1986].

Single cell cultures are especially appropriate for studying intracellular mechanisms coupled to the activation of receptors located in the cell membranes. In addition, the details of regulated exocytosis of hormone-containing granules can be studied. However, this does not result in much information about the integrated

communication and regulation between cells. In addition, the cells are not very viable. Both β and α cells can be purified from cell cultures, but the α cells are often contaminated by surrounding γ cells. Moreover, the islets are not very rich in α cells, so after isolation the amount of cells is often quite low. The β cells are more numerous than α cells, and thus provide a higher amount following isolation.

In the perfused small intestine model, the experimental setup enables to differentiate between luminal and vascular stimuli, which is crucial for localizing sites of stimulation. Additionally, isolation and perfusion of the colon ensures that the impact from other sites of the organism, that would otherwise produce a secondary effect disturbing the result, is prevented. Importantly, degradation of hormones and test substances by whole-body metabolism is also avoided and the exact concentration reaching the organ can be calculated accurately.

In conclusion, *in vivo* experiments allow studies of blood-borne factors, since the natural anatomy and natural perfusion is not disturbed. Nevertheless, it is very difficult to study the dynamics of secretion in small rodents and especially intra-islet mechanisms *in vivo* [Holst JJ et al, 2011].

3.2.1. In situ perfused rat pancreas

Handling of the animals was performed in accordance with international guidelines (1987), and experiments were carried out with permission from the Danish Animal Experiments Inspectorate (2013-15-2934-00833) and the local ethics committee (EMED, P-15-408). Male Wistar rats (250-300g), approximately 8 weeks of age, were purchased from Janvier labs (Le Genest-Saint-Isle, France) more than one week before experiments were performed and given free access to standard rodent chow and water. Animals were housed 2 per cage under a 12:12-h light-dark cycle.

The rats were anaesthetised with a subcutaneous injection of Hypnorm/Midazolam (0.0158 mg fentanyl citrate + 0.5 mg fluanisone + 0.25 mg midazolam / 100 g), and supplemented with half the dose for every 30 min if more time was needed. After lack of reflexes was established, the operation was started by opening the abdomen and the intestine pulled aside to expose the pancreas [Deacon CF et al, 2006].

For perfusion the catheter is inserted in aorta, thereby perfusing the pancreas through the superior mesenteric artery and celiac arteries. However, the small intestine, spleen and stomach are also perfused through the two arteries; thus, to circumvent this, we ligated their blood supply and removed the organs. All vessels were ligated using suture.

The draining catheter was placed into the vena portae as close to the liver as possible, and recirculation with perfusion buffer was started. The flow was adjusted to 4 ml/min. Proximal to the portal catheter, vena portae and the bile duct were also ligated, and a small hole was cut in the distal part of the duodenum for drainage. Finally, cutting into diaphragma killed the rat. Moreover, euthanasia of the animal prevented stress responses that might have affected the experiment. For overview of the perfusion setup see Figs. 3 and 4.

Fig. 3. The catheter at the bottom of the picture is placed in the aorta, and provides the pancreas with perfusion buffer. The catheter at the top collects the effluent. Pancreas appears pale because of the clear perfusion buffer

Fig. 4 Overview of the perfusion setup. The buffer was oxygenated and then pumped through the heating chamber and the bubble trap. A fraction collector (barely visible at the bottomleft in this picture), collected the effluent.

A scheme of the perfusion setup can be seen in Fig. 5. We used equipment dedicated for rodent organ perfusion (Hugo Sachs Elektronik, March-Hugstetten, Germany). The system includes a heating plate, a pump, a bubble trap, a water bath of 37°C, a syringe infusion pump and a pressure gauge. The pancreas was perfused using a modified Krebs-Ringer bicarbonate buffer containing in addition 5% dextran T-705% dextran T-70 (Pharmacosmos, Holbaek, Denmark), 0.1% human serum albumin, 10 mM or 7 mM glucose, and 5 mM pyruvate, fumarate and glutamate. Prior to the experiment the buffer was filtered to remove possible contaminations.

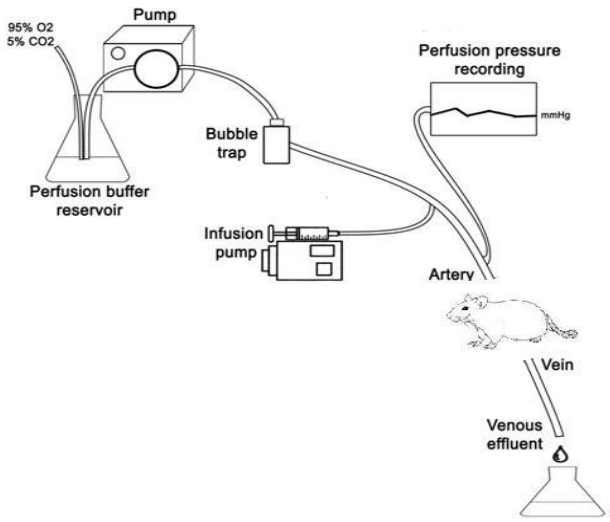

Fig 5. Schematic overview of the perfusion setup. Oxygenated perfusion buffer is collected from a glass reservoir and pumped through a bubble trap and then into the pancreas. Different substances can be added through the infusion pump. The effluent is collected and kept on ice until frozen at -20°C. Perfusion pressure is recorded on a connected computer.

The perfusion buffer was heated to approximately 37°C and continuously gassed throughout the experiment with 95% O_2 and 5% CO_2 using a glass frit placed in the perfusion buffer reservoir to achieve pH 7.4 and a high oxygen partial pressure. During an equilibrium period of 20 min baseline samples were collected each minute, and afterwards ABA was infused into the arterial vascular supply to reach the final concentrations of 1, 10 or 100 µM for 10 min periods, separated by baseline periods allowing hormone secretion to stabilize before and after stimulation. A 5-minute L-Arginine (10 mM) infusion was included at the end of each experiment as a positive control of hormone response. ABA and L-Arginine were added at a flow rate of 0.2 ml/min. Samples were collected from the portal vein at 1 min intervals, and stored at -20°C until analysis.

3.2.2. In situ perfused proximal small intestine

The experimental method and protocol have been described elsewhere in detail [Kuhre RE et al, 2014]. In brief, non fasted male Wistar rats (weight: 300-320 g) were anesthetized with a subcutaneous Hypnorm/Midazolam injection and placed on a 37°C heating plate. The abdominal cavity was opened; the entire large intestine and the distal half of the small intestine was carefully removed, leaving 42 ± 3 cm of the upper small intestine in situ (approximately half of the entire small intestine). A plastic tube was inserted into the proximal part of the lumen and the intestinal content was carefully removed by flushing with isotonic saline. Next, the lumen was perfused with saline at a steady flow of 0.5 mL/min. A catheter was placed in the superior mesenteric artery and the intestine was vascularly perfused with perfusion buffer with the same composition of the buffer used to perfuse pancreas (see above), plus 10 µmol/L 3-Isobutyl-1-methylxanthine (IBMX) (Sigma-Aldrich, cat. no. 5879), 2 mL/L Vamin (cat. no. 11338; Fresenius Kabi, Uppsala, Sweden), and 3.5 mmol/L glucose, (95% O_2−5% CO_2), warmed to 37°C at a rate of 7.5 mL/min. The rats were sacrificed by cardiac perforation and after an equilibration period of 30 min, perfusion effluent was collected each minute from a catheter inserted in the vena portae and samples kept on ice and stored at −20°C until analysis. ABA was luminally infused into the proximal part of the lumen and vascularly into the arterial vascular supply to reach the final concentrations of 200 µM for 10 min periods, separated by baseline periods allowing hormone secretion to stabilize before and after administration. A 5-minute infusion with Bombesin (10 nM) was included at the end of each experiment as a positive control of hormone response.

3.2.3. Hormone analysis

Insulin and GLP-1 concentrations in the venous effluent were analyzed using a radioimmunoassay (RIA). RIA is a technique based on immunological reactions between an antibody and an antigen, combined with radioactive labeling to determine low concentrations of antigenic substances.

Insulin concentrations were determined using guinea pig antiserum raised against porcine insulin (2006-3), which strongly cross-reacts with both insulin I and II. A standard solution obtained from Peninsula was used to generate the standard curve.

GLP-1 concentrations in the venous effluents were determined using a rabbit antiserum directed against the C-terminus of GLP-1 (code no. 89390), thus reacting with all amidated forms of GLP-1 (1-36NH2, 7-36NH2 and 9-36NH2).

3.2.4. Detection of ABA by ELISA

The amount of ABA in the effluent samples was measured by ELISA, see above 3.1.8.

3.2.5. Statistical analysis and graphic presentation of perfusion experiment

Data are expressed as means ± SEM or SD. Statistical analysis of hormone secretion was performed by a comparison of the mean basal level 10 min prior to the infusion and the mean output during the 10 min of infusion.

Statistical significance levels were tested using a paired *t*-test. All statistics were performed using Graphpad Prism 7 program (La Jolla, CA). $P < 0.05$ was considered significant. Sample size (*n*) was at least 5 or 6 in the different experiments.

3.3. Effect of ABA on cell survival and NO production in N2a cells

3.3.1. Determination of nitrite in N2a cells

Murine neuroblastoma N2a cells were maintained in Dulbecco's modified Eagle's culture medium (DMEM) supplemented with 10% fetal bovine serum and penicillin/streptomycin in a humidified atmosphere containing 5% CO_2 at 37°C.

N2a cells (500,000 cells/well) were seeded in 6-well plates. After 24h, the culture medium was removed and the cells were pre-incubated at 37°C for 1h in Hank's balanced salt solution (HBSS) with 1 mM Arginine. Cells were then washed 3 times with 1ml HBSS and then stimulated at 22°C in triplicate without or with 10 µM ABA for 0, 5, 10, 20 min. Nitrite content was determined using 10 µM 2,3-diaminonaphthalene (DAN) to form the fluorescent product 1-(H)-naphthotriazole, as described [Misko S et al, 1993].

3.3.2. Hypoxia

N2a cells (500,000 cells/well) were seeded in 25 cm^2 culture flasks. After 24h, the culture medium was removed, cells were washed 2 times with HBSS. Cells were pre-incubated at 37°C for 1h in HBSS with or without 10 µM ABA and with or without the eNOS inhibitor L-NAME (100 µM) and then subjected to normoxic culture conditions or to hypoxia. To induce hypoxia (<2% O_2) cells were subjected to 30 min of continuous nitrogen flushing, as described by Keira and collegues [Keira SM et al, 2004]. Briefly, 25 cm^2 culture flasks with 2 ml of HBSS were closed with silicon stoppers and sealed with a double layer of cellulose film (Parafilm M®); nitrogen flushing was maintained for 30 minutes with a constant flow and then the culture flasks were kept sealed at 37°C in the incubator. After 6h of incubation, cell viability was determined by Trypan blue exclusion.

3.3.3. Western blot analysis

The cell pellets were lysed in H_2O in the presence of a protease inhibitor mixture for mammalian cells (Sigma). The lysates were sonicated 3 times for 30s on ice and the protein concentration was estimated with the Bradford assay. After SDS-PAGE, Western blot analyses were performed using nitrocellulose membranes (Bio Rad) according to the standard method (see above, paragraph 3.1.6) The used antibodies were as follows: anti-p-ERK 1/2 (Santa Cruz, CA, USA), anti-mouse IgG antibody for vinculin (kindly provided by Prof. Emilia Turco, University of Turin, Italy).

3.3.4. Statistical analysis.

Data are expressed as means ± SD. Statistical significance was tested using a paired *t*-test. All statistics were performed using Graphpad Prism 7 program (La Jolla, CA). $P< 0.05$ was considered significant. Sample size (*n*) was at least 2 in the different experiments.

4.0 Results

4.1. ABA stimulates GLP-1 release from L-cells both *in vitro* and *in vivo*

4.1.1. ABA stimulates GLP-1 secretion from an enteroendocrine cell line

The human L cell line hNCI-H716 was challenged for 2 h with different ABA concentrations and GLP-1 levels were measured in the supernatants. The basal GLP-1 concentration was 347 ± 106 pM. As shown in Fig.6A, 200 µM ABA approximately doubled the extent of the GLP-1 secretion. 10 µM ABA was sufficient to trigger a statistically significantly higher GLP-1 release, compared to the untreated control. No stimulation of GLP-1 secretion was obtained in the presence of 100 nM ABA. The calculated EC50 for the ABA-induced GLP-1 release was 23 ± 3 µM (not shown). To compare the effect of ABA on GLP-1 release with that of other secretagogues, cells were also incubated in the presence of 200 mM glucose or 10 mM glutamine [Jang HJ et al,2007; Reimann F et al, 2004]: GLP-1 secretion was increased by approximately 1.4-fold with both stimuli (Fig. 6A).

Interestingly, ABA treatment also significantly increased preproglucagon mRNA levels, as demonstrated by qPCR using two different sets of primers, specific for GLP-1 and glucagon, respectively, yielding a similar result (Fig. 6B).

4.1.2. The ABA-induced GLP-1 secretion is mediated by a cAMP-dependent mechanism

In different human cell types, the cell-specific ABA-induced response is mediated by an increase of the second messenger cAMP and by the consequent PKA activation [Bruzzone S et al, 2007, 2008; Sturla L et al, 2009; Bassaganya-Riera J et al, 2011; Guri

AJ et al, 2010 (b]. Since GLP-1 release is regulated by the $[cAMP]_i$ [Ezcurra M et al, 2013], we verified whether ABA was able to induce an increase of the $[cAMP]_i$ in hNCI-H716 cells. As a positive control, cells were incubated with glutamine, which is known to determine a $[cAMP]_i$ increase in hNCI-H716 cells [Tolhurst G et al, 2011]. As shown in Fig. 7A, a 2.5-min incubation in the presence of 200 µM ABA induced a 2-fold increase of the $[cAMP]_i$, while 10 mM glutamine increased the $[cAMP]_i$ approximately 1.4-fold.

In mammalian cells, the ABA-induced cAMP increase is mediated by the protein LANCL2 [Sturla L et al, 2009; Bassaganya-Riera J et al, 2011]. hNCI-H716 cells were transfected by electroporation with an empty plasmid, or with a plasmid containing the full-length cDNA for human LANCL2. LANCL2 overexpression, confirmed by Western blot analysis with a specific monoclonal antibody (Fig. 7B), was accompanied by a significant increase in ABA-induced cAMP accumulation, as compared to cells transfected with an empty plasmid (Fig. 7C), as well as by a significant increase in ABA-induced GLP-1 release (Fig. 7D). The ABA-induced $[cAMP]_i$ increase and GLP-1 release were approximately 1.4-fold in cells transfected with the empty plasmid (control bars in Fig. 7D), and not 2-fold as observed in untransfected cells (Figs. 6B and 7A), indicating that cell responsiveness was slightly affected by the transfection procedure *per se*.

In order to verify whether the ABA-induced $[cAMP]_i$ increase mediates the ABA-stimulated GLP-1 release, hNCI-H716 cells were pre-incubated in the presence of a specific adenylyl cyclase inhibitor (2',3'-Dideoxyadenosine), or a cell permeable PKA inhibitor: both inhibitors abrogated the GLP-1 release stimulated by 200 µM ABA (Fig. 6A).

4.1.3. ABA increases plasma GLP-1 in rats

First, we examined the effect of a single oral dose of ABA (at 50 mg/Kg) on GLP-1 levels in normal rats (6 animals per experimental group) pre-treated with Sitagliptin. 20 min after ABA administration, plasma GLP-1 (GLP-1p) increased by approximately 50%, whereas the vehicle alone had no effect on GLP-1p levels (Fig. 8A). The area under the curve of GLP-1p (GLP-1p AUC) over the entire time-frame was calculated from GLP-1p values relative to time zero: the GLP-1p AUC was significantly higher in the ABA-treated compared to the control animals (Fig. 8B).

GLP-1 levels also significantly increased in the portal vein blood of rats not pre-treated with Sitagliptin 10 min after ABA administration indicating that ABA alone is capable of increasing plasma GLP-1. ABA concentration in the portal vein blood was in the low nM range (4.2 ± 1.9 nM) in the vehicle-treated animals and in the μM range (3.9 ± 0.4 μM) in the ABA-treated animals.

The observation that ABA induced an increase of GLP-1p, together with the fact that exogenous ABA is known to directly stimulate insulin release from β-cells *in vitro* [Bruzzone S et al, 2008], prompted us to measure insulin levels in the ABA-treated rats. As shown in Fig. 8C and 8D, insulinemia indeed significantly increased after ABA administration and the plasma insulin AUC was consequently higher in the ABA-treated than in the vehicle-treated group.

Glycemia was slightly increased in vehicle-treated animals: this increase was not observed upon oral ABA administration (Figs. 8E and 8F). The increase of glycemia observed in the control animals can be attributed to anesthesia: indeed, ketamine/xylazine have been shown to induce hyperglycemia in fed rats and, to a lower extent, also in fasted animals [Saha JK et al, 2005], as in our experimental protocol.

In conscious rats, oral ABA administration at the same dose used in the anesthetized animals (50 mg/Kg) resulted in a slight, yet significant reduction of blood glucose after 60 min (81 ± 6 mg/dL, n = 6) compared with time zero values (92 ± 10, n = 12, p = 0.03) and with values measured at the same time point in the vehicle-treated controls (99 ± 14, n = 6; p = 0.02)

4.2. Insulin, GLP-1 and ABA release in the perfused pancreas and proximal small intestine rat model

4.2.1. ABA stimulates insulin secretion from perfused rat pancreas

Rat pancreas perfused with 10 µM or 100 µM ABA showed a significant increase of insulin secretion compared to baseline values (Fig. 9A). Specifically, the area under the curve (AUC) increased from 10.2 ± 0.8 (calculated from 1 to 10 min) to 13.6 ± 2.3 (calculated from 11 to 20 min) in rats perfused with 10 µM ABA (Fig. 9B); the AUC increased from 10.8 ± 0.3 (calculated from 31 to 40 min) to 16.7 ± 19 (calculated from 41 to 50 min) in rats perfused with 100 µM ABA (Fig. 9C). In this experimental setting, ABA failed to induce a significant release of insulin at a concentration of 1 µM. At the end of all experiments, Arginine was administered as a positive control.

These results are in line with our previous studies, showing that ABA induces the release of insulin in a dose-dependent fashion.

4.2.2. GLP-1 stimulates the release of ABA from the perfused rat pancreas

Next, rat pancreas was perfused with GLP-1, which was previously shown to evoke ABA release from beta-pancreatic cells [Bruzzone S et al, 2012 (a]. Upon perfusion with GLP-1 in a high-glucose buffer, both ABA and insulin concentrations were evaluated in the collected samples. As expected, 1 nM GLP-1 evoked insulin secretion

(Fig. 10A). Indeed, upon GLP-1 infusion, ABA was also released, together with insulin: the ABA concentration increased in a biphasic manner, from a basal value of approximately 4.5 to 15.0 and 9.9 pmol/ml, after 3 and 11 min after GLP-1 infusion, respectively (Fig. 10B). Notably, a positive correlation was found between the ABA AUC and the insulin AUC upon GLP-1 administration ($r=0.84$, $p<0.05$, $n=6$).

4.2.3. ABA stimulates GLP-1 secretion from the perfused rat proximal small intestine and is absorbed into the circulation

Vascular administration of 200 µM ABA in the perfused rat proximal small intestine significantly increased the venous effluent GLP-1 concentration: the baseline AUC of GLP-1, calculated from 26 to 35 min, was 224.0 ± 61.1 pmol/L and the AUC of GLP-1 after infusion of ABA calculated from 36 to 45 min, was 381.3 ± 129.9 pmol/L (*$p=0.048$; Figs. 11A and 11B). In contrast, luminal administration of 200 µM ABA did not appear to significantly affect GLP-1 secretion: the baseline AUC of GLP-1, calculated from 1 to 10 min, was 235.6 ± 38.2 pmol/L and the AUC of GLP-1 after perfusion with luminal ABA, calculated from 11 to 20 min, was 351.4 ± 21.6 pmol/L ($p>0.05$; Fig. 11C). In all experiments, bombesin (BBS) was intravascularly administered as a positive control. In order to verify that luminal ABA is adsorbed in this experimental settings, the vascular ABA concentration upon luminal administration of 200 µM ABA was measured. Indeed, already after 1 min from its luminal administration, ABA was present at micromolar concentrations in the vascular effluent. After 4 min from luminal ABA perfusion, the final ABA concentration in the venous effluent was approximately 5 µM (Fig. 12).

4.3 ABA improves survival of N2a cells to hypoxia through the stimulation of eNOS

4.3.1. ABA stimulates NO production by N2a cells

N2a cells were incubated under normoxic conditions without (control) or with 10 µM ABA and nitrite accumulation in the supernatant was measured with the fluorescent probe 2,3-diaminonaphthalene (DAN). ABA stimulated NO release by N2a cells, with an approximately two-fold increase over control cells observed after 5,10, 20 min incubation with 10 µM ABA(*p<0,05) (Fig. 13).

4.3.2. ABA improves cells survival to hypoxia via NO

After 6h of hypoxia, cell mortality was approximately 55% compared with normoxic conditions. N2a cultures pre-incubated with 10 µM ABA showed a significant increase (*p<0,02) in cell survival compared with control cultures, not pre-incubated with ABA under hypoxia condition (Fig. 14). Pre-treatment of the cells with L-NAME abrogated the ABA-induced rescue of the cells from hypoxia-induced death (**p<0,01) (Fig. 14).

4.3.3. ABA induces upregulation of p-ERK in N2a cells under hypoxia

Several studies have demonstrated that the MAPK/ERK pathway plays a role in neuroprotection. To determine whether ABA regulates the MAPK/ERK pathway, we investigated the expression and phosphorylation levels of ERK in N2a cells cultured under hypoxia.

Levels of p-ERK were significantly increased in N2a cells exposed to hypoxia, as compared with normoxic conditions, both at 1h and 6h; presence of 10 µM ABA during hypoxia further significantly increased p-ERK expression compared with normoxic cells. (Fig. 15). (*p<0,05). No difference in p-ERK expression was registered between cells treated with ABA and without ABA under hypoxia condition.

5.0 Discussion

The number of people with T2DM is rapidly growing in both developed and developing countries. In the US, it is estimated that 10% of the present population aged between 20 and 79 is affected by T2DM and in Asia, where the percentage of diabetic subjects was negligible in the year 2000, it has risen to 7.6% of the population in 2010 and will further increase to 9.1% in 2030, according to the International Diabetes Federation. This would mean that approximately 450 million people will be affected by T2DM in the world by the year 2030 [Chamnan P et al, 2011]. These numbers demand an intense search for effective therapeutic strategies to combat T2DM.

Over the past decade, several studies have unveiled the role of ABA in mammals as a new hormone involved in the regulation of glycemia, suggesting its possible use in T2DM prevention and treatment.

Emerging anti-diabetic therapies rely heavily on GLP-1 mimetics and any new information regarding the physiology of endogenous GLP-1 will be important to improve its therapeutical use. The observation that GLP-1 stimulates ABA release from β-pancreatic cells [Bruzzone S et al, 2012 (a] can now be further extended by results obtained in this thesis, demonstrating that ABA can also induce GLP-1 release, both *in vitro* and *in vivo*. Together, these results indicate presence of a positive feed-back mechanism between ABA and GLP-1, which may be relevant to the physiology of glycemia regulation and may also be explored as a means to improve endogenous GLP-1 function.

The molecular mechanism by which ABA induces GLP-1 release by hNCI-H716 cells is similar to the one described in several other cell systems (including immune cells, β-pancreatic cells and endothelial cells), i.e. through the cAMP/PKA axis [Bruzzone S et

al, 2007 and 2008; Tossi V et al, 2012; Sturla L et al, 2009; Bassaganya-Riera J et al, 2011; Guri AJ et al,2010 (a and (b]. Indeed, this signaling pathway is known to regulate GLP-1 release also in response to other stimuli, such as glucose and glutamine [Ezcurra M et al, 2013; Sandoval DA et al, 2015; Tolhurst G et al, 2011].

In the *in vivo* experiments, we chose to administer a dose of ABA of 50 mg/Kg, based on the results obtained by Guri [Guri AJ et al, 2007], showing that dietary ABA at 100 mg/Kg, introduced over a 24-h period, was effective in reducing glycemia in db/db mice fed a high-fat diet. We hypothesized that a smaller dose could also be effective, if bolus-administered by gavage.

The increase of plasma insulin upon ABA administration was expected, based on the *in vitro* effect of ABA on insulinoma cells and on murine and human β-cells: exogenous ABA, added at concentrations in the low nM range, stimulated insulin secretion both in the presence and absence of glucose [Bruzzone S et al, 2008]. The plasma ABA concentration measured in the rats 10 min after oral ABA administration was in the micromolar range and could thus be responsible for the observed increase of plasma insulin (Fig. 8C). The increase of plasma GLP-1 peaked at 20 min (Fig. 8A), preceding the insulin increase (which conversely was maximal at 40 min, Fig. 8C). Indeed, detection of high GLP-1 levels in the portal vein upon ABA administration demonstrates that oral ABA alone is capable of increasing plasma GLP-1 (Fig. 8A).

In control animals, glycemia was significantly higher at both 20 and 40 min compared with time zero. The increase of glycemia observed in the control animals might be attributed to anesthesia, as described by Saha [Saha JK et al, 2005], who showed that ketamine and xylazine significantly altered glycemia in fed and, to a much lower extent, also in fasted rats, as occurred in our study (Fig. 8E, white squares).

In ABA-treated rats, the increase of glycemia was not observed, neither at 20 nor at 40 min (Fig. 8E, black squares): while, at 40 min, a significant increase of insulinemia (Fig. 8C) may have contributed to glycemia control, at 20 min insulinemia was not

(yet) increased. Thus, two mechanisms may be responsible for the maintenance of normal blood glucose levels in the ABA-treated, anesthetized animals: i) an “early” (0-20 min), insulin-independent glycemia lowering effect of ABA, followed by, ii) a “late” (20-40 min) glycemia reducing effect, attributable to the increase of insulinemia. We previously reported that ABA can trigger glucose uptake in myocytes and in adipocytes [Bruzzone S et al, 2012 (a], to a similar extent as that observed with insulin at the same concentration (i.e. 100 nM). Thus, the normalization of glycemia observed in the ABA-treated animals compared with the controls could result from stimulation by ABA of both glucose transport and insulin release. The plasma concentration of ABA measured 10 min after its administration, which was in the micromolar range, was markedly higher than the one capable of stimulating myoblast glucose uptake *in vitro* [Bruzzone S et al, 2012 (a].

Results obtained on isolated cells were confirmed and extended in the perfused pancreas and small intestine experimental system.

Indeed, infusion with 10 µM and 100 µM ABA stimulated insulin release in the perfused rat pancreas. These data confirm previous results obtained with human pancreatic islets, RIN-m and INS-1 insulinoma cells [Bruzzone et al, 2008], demonstrating that ABA stimulates insulin release in the low nanomolar range. In the perfusion model, ABA stimulated insulin release at higher concentrations, with 1 µM being not effective, indicating a lower sensibility for this experimental setting to register ABA-induced responses. This observation may be in line with results obtained in the *in vivo* setting: ABA induced insulin release when orally administered at 50 mg/Kg in fasted rats [Guri AJ et al, 2007]. Conversely, microgram amounts of ABA improved the glycemic profile without increasing insulinemia in rats and in healthy humans undergoing an oral glucose tolerance test [Magnone M et al, 2015].

Moreover, we demonstrated on the isolated perfused rat small intestine that ABA induced GLP-1 release upon vascular perfusion, while luminal stimulation with ABA

did not evoke a detectable GLP-1 release. However, as mentioned above, ABA stimulated GLP-1 release in an *in vivo* model, where plasma GLP-1 increased after a single-dose oral administration of ABA in fasted rats, indicating that luminal ABA is effective in releasing GLP-1, either by acting directly from the lumen, or after its absorption. It was shown that vascular, but not luminal, administration of linoleic acid stimulates GLP-1 release from isolated rat small intestine: linoleic acid is an essential fatty acids, that the human body cannot synthesize and must be taken with the diet and absorbed by the intestine [Christensen LW et al, 2015]. Thus, it is possible that ABA behaves similarly to linoleic acid and stimulates GLP-1 release acting on the vascular side only of the L-cells. Nevertheless, it should also be noted that application of 100 μmol/L taurodeoxycholate (TDCA), via the vasculature, in perfused rat small intestine, robustly increased GLP-1 release, whereas luminal application of TDCA at the same concentration was significantly less effective. A much higher concentration of TDCA (1 mmol/L) was needed to stimulate GLP-1 secretion [Brighton CA et al, 2015]. Our results indicate that ABA is more effective, at least in this experimental setting, when acting from the vascular side compared to the luminal side: a direct effect of luminal ABA, *in vivo,* on GLP-1 release cannot be excluded.

Interestingly, we demonstrate that GLP-1 stimulates ABA release from the perfused rat pancreas (Fig. 10). This result is in line with our previous observation, obtained using the insulinoma cell line INS-1, that GLP-1 stimulates ABA release from β-pancreatic cells, in the presence of both a low or a high glucose concentration [Bruzzone S el at,2012 (a]. Notably, a positive correlation was found between the ABA AUC and the insulin AUC upon GLP-1 administration, suggesting: i) a cooperation between ABA and GLP-1 in insulin release; ii) the possibility that endogenous ABA might be necessary to stimulate the GLP-1-induced insulin release.

In conclusion, ABA induces GLP-1 secretion from L cells, GLP-1 stimulated ABA and insulin secretion in β-cells and ABA induces insulin secretion in this cell type, indicating a cross-talk between GLP-1 and ABA.

Future studies should explore the effect of GLP-1 analogues or DPP-IV inhibitors on the release of endogenous ABA.

Identifying LANCL2-activating compounds might indeed prove a successful strategy, in view of the multiple anti-diabetic effect that they might trigger. The potential role of LANCL2 as a new drug target in diabetes has recently been suggested [Lu P et al, 2014].

So far, it is not possible to exclude that, when administered *in vivo*, ABA can also trigger GLP-1 release from organs/tissues other than L-type cells, e.g. β-pancreatic cells [Sandoval DA et al, 2015]. Moreover, it is not possible to exclude that ABA stimulates GLP-1 from the luminal side of L-cells, like a nutrient; interestingly, ABA can stimulate GLP-1 release from the vascular side of the L-cells, as an endogenous hormone.

Finally, results presented in this thesis contribute new information on the role of ABA in the hormonal cross-talk between insulin and GLP-1, which lies at the heart of glycemia homeostasis. These results provide a strong rationale for testing the possibility of exploiting ABA as a new anti-diabetic drug, possibly in combination with GLP-1 mimetics, in the clinical setting.

Furthermore, GLP-1 has neuroprotective effects: thus, impairment of the ABA-GLP-1 cross-talk in T2DM may contribute to the increased incidence of neurological complications in T2DM patients. Indeed, the results obtained with ABA on the neuroblastoma cell line N2a support the conclusion that ABA plays a role in the protection of neuronal cells to hypoxia, a condition which frequently occurs in the diabetic tissues due to microvascular damage. We demonstrated that ABA stimulates

NO release from N2a cells, and this result is in line with previous observations that ABA induced NO release in microglia, human granulocytes and keratinocytes [Bruzzone S et al, 2012 (b and 2007; Bodrato N et al, 2009].

Indeed, we demonstrated that ABA improves N2a survival to hypoxia and this event is NO- and NOS-dependent. ABA increases cell survival to hypoxia by 30% compared to untreated cultures, and this effect is abrogated by the NOS inhibitor L-NAME. This result suggests a neuroprotective role of ABA under hypoxic conditions.

NO is an important signaling molecule that is widely used in the nervous system. Evidence suggests that after an ischemia/reperfusion injury, stimulation of eNOS and increase in NO generation occur and that this signalling pathway plays an essential neuroprotective role in the regulation of cerebral blood flow [Garry PS et al, 2015].

Furthermore, we demonstrated that ABA induces the phosphorylation of ERK1/2 in N2a cells under hypoxia condition, suggesting a role for p-ERK in the ABA-induced activation of eNOS. These results are in line with a study conducted by Liu XW [Liu XW et al, 2015], where they demonstrate that melatonin prevented hypoxia-induced apoptosis in N2a cells by activating the ERK pathway. In cerebral endothelial cells, resveratrol promotes angiogenesis via NO/eNOS and this signalling is mediated by p-ERK [Simão F et al, 2012]

Based on the results obtained with ABA on neuroblastoma cells, we propose that ABA may indeed participate to neuronal protection against hypoxia by stimulating neuronal NO generation via the activation of the pERK/eNOS pathway: it remains to be established whether stimulation by ABA of NO synthesis might occur also on cerebral endothelial cells.

II CHAPTER

1.0 Introduction

1.1. White and brown adipose tissues

During the past two decades, the incidence of obesity and type 2 diabetes mellitus (T2DM) has increased rapidly worldwide and a cause-effect relationship between the two conditions has been established. Consequently, interest has grown to elucidate the molecular mechanisms underlying the diabetogenic role of obesity.

In mammals, two different types of adipose tissue (AT) are present, which have essentially different functions: the white AT (WAT) stores excess energy as triglycerides; conversely, the brown AT (BAT) is specialized in the dissipation of metabolic energy through the production of heat.

WAT has long been recognized as the main site of storage of excess energy derived from food intake [Rosen ED et al, 2006]. White adipocytes (the predominant cell type in white adipose tissue) store dietary energy in a highly concentrated form as triglyceride, mostly in a single large lipid droplet. These triglycerides can be rapidly hydrolysed by lipases and the resulting fatty acids are transported to other tissues to be oxidized in mitochondria as an energy source. The first indication that adipose tissue also functions as an endocrine organ was the discovery of leptin production by adipocytes. Adipose tissue secretes a large number of peptide hormones and cytokines and also activated lipids [Kershaw EE et al, 2004].

In a normal healthy subjects, when energy intake is scarce, triglycerides stored in the WAT can be hydrolysed and the fatty acids are released as into the blood stream,

where they can be taken up by other tissues (e.g. liver and skeletal muscle) and used as an energy source. When energy intake consistently exceeds energy expenditure, the AT expands due to hypertrophy, but also due to hyperplasia of the adipocytes.

By contrast, BAT is specialized primarily in non-shivering thermogenesis, a cold climate adaptation in many homeotherms [Smith RE et al, 1969]. Brown adipocytes are characterized by multiple, smaller droplets of triglycerides, which are accessible for rapid hydrolysis and rapid oxidation of the fatty acids. A high content of mitochondria (responsible for the brown colour) and the presence of the uncoupling protein-1 (UCP-1) allow the use of the metabolic energy derived from fatty acid oxidation for the generation of heat. Significant depots of brown fat are found in rodents and in other hibernating mammals, and also in newborn infants. Recent investigations, have shown that human adults also have metabolically active BAT and that BAT may indeed play an important role in energy homeostasis in adults [Gesta S et al, 2007]. Human BAT is activated by acute cold exposure, by beta-adrenergic stimulation and by thyroid hormones, all of which stimulate energy expenditure. The metabolic activity of BAT is lower in older and obese individuals. The inverse relationship between BAT activity and (white) body suggests that BAT, because of its energy dissipating activity, is protective against body fat accumulation.

WAT mass, and thus the body-mass-index, largely depends on the balance between lipid storage and utilization, which is challenged under conditions of excess food intake. Major pathological consequences of overnutrition and obesity result from an increase in lipid flux to non-adipose organs and the development of insulin resistance.

1.2. GLUT-4

GLUT4 (glucose transporter 4) plays a pivotal role in insulin-induced glucose uptake to maintain normal blood glucose levels. GLUT4 transporters are insulin sensitive, and are predominantly expressed in skeletal muscle and AT, where they are responsible for the post-prandial uptake of excess glucose from the bloodstream.

In the absence of insulin, GLUT4 is stored in intracellular vesicles. In response to acute insulin stimulation, these vesicles translocate to the plasma membrane, resulting in the redistribution of GLUT4 to the plasma membrane, where it facilitates glucose uptake.

The signal transduction pathway initiated by insulin to translocate GLUT4 and increase glucose uptake has been extensively studied, and two signal transduction pathways have been identified in this process. One is the insulin receptor substrate (IRS)-phosphatidylinositol (PI) 3-kinase-dependent pathway, in which activated phosphatidylinositide 3-kinases (PI3K) in turn activates downstream signaling molecules, such as PDK1 and Akt [Huang S et al, 2007].The other mechanism is the de-repression of GLUT4 transcription by removal of bound PPARγ from the GLUT4 promoter by PPARγ ligands (such as the antidiabetic drugs thiazolidinediones, TZDs).

Insulin resistance arises when glucose uptake by muscle and AT is reduced in response to insulin, and it is associated with the pathophysiology of T2DM. Indeed, insulin resistance in AT is caused by impaired initial-phase insulin signaling and reduced GLUT4 levels. A central role for GLUT4 in whole-body metabolism is strongly supported by a variety of genetically engineered mouse models where expression of the transporter is either enhanced or ablated in muscle or AT or both. Indeed, in mice lacking GLUT-4 in adipocytes, a systemic insulin resistance is observed [Favaretto F et al, 2014; Wallberg-Henriksson H et al, 2001]. This *in vivo* evidence suggests that adipocyte glucose metabolism is critical to whole-body glucose homeostasis.

1.3. PPARγ

The family of peroxisome proliferator-activated receptors (PPARs) comprises several nuclear receptors characterized as adopted orphan receptors, which are activated by a variety of fatty acids and their derivatives, such as prostaglandins [Desvergne B et al, 1999]. PPARγ is the master transcription factor regulating adipogenesis. This receptor is known to be obligate for adipocyte differentiation [Rosen ED et al, 1999] and its overexpression/activation is in many cases sufficient to convert non-adipose cells to adipocyte-like cells.

PPARγ also induces PGC-1α, and promotes transcription of UCP-1, the key marker of BAT. UCP-1 is specifically expressed in the inner membrane of mitochondria from brown adipocytes to generate heat by uncoupling oxidative phosphorylation [Tiraby C et al, 2003].

1.4. ABA and AT

As mentioned in the first Chapter, ABA plays a role in the regulation of glycemia by stimulating GLP-1 and insulin release and by promoting glucose transport in GLUT4-expressing cells, which include muscle and AT.

Indeed, several observations suggest that the AT could be a metabolic target of ABA. ABA activates PPARγ *in vitro* in the murine pre-adipocyte cell line 3T3-L1 and dietary ABA-supplementation increases PPARγ-responsive gene expression and reduces white adipose tissue inflammation in mice [Guri AJ et al, 2007]. Moreover, ABA treatment improves insulin sensitivity, decreases adipocyte hypertrophy, reduces macrophage infiltration into the WAT, and down-regulates the levels of the inflammation markers tumor necrosis alpha (TNFα) and MCP-1 in obese mice [Guri AJ

et al, 2008]. Human adipose tissue releases ABA in response to high glucose and nanomolar ABA stimulates glucose uptake, similarly to insulin, in 3T3-L1 cells differentiated to adipocytes, by increasing GLUT-4 translocation to the plasma membrane [Bruzzone S et al, 2012 (a].

2.0 Aim of the study

Obesity represents a major medical and societal challenge, due to its associated morbidity, particularly insulin resistance and T2DM. Over the past 10 years, several studies were conducted to elucidate the molecular mechanisms through which excess adipose tissue predisposes to the development of T2DM, aiming at developing new therapeutic approaches for the prevention of obesity and of obesity-related metabolic diseases.

We hypothesized a role for ABA as an endogenous hormone in the AT, based on the observations that: i) ABA is released from human adipose tissue (AT) stimulated with high glucose concentrations; ii) ABA stimulates GLUT4 translocation to the plasmamembrane in mouse pre-adipocytes [Bruzzone S et al, 2012 (a] and iii) ABA activates PPARγ, the transcription factor presiding over adipogenesis [Guri AJ et al, 2007].

For this reason, we investigated the role of the ABA/LANCL2 system in the regulation of glucose uptake, in the metabolic fate of the internalized glucose and in the transcription of specific genes involved in adipogenesis and browning in rodent and human adipocytes.

3.0 Materials and Methods

3.1. Materials

Dulbecco's modified Eagle's culture medium (DMEM) was purchased from Euroclone SpA (Milano, Italy) and the Fetal Calf Serum (FCS) was from LGC Standards (Milano, Italy). Lipofectamine 2000 was purchased from Lonza (Milano, Italy). [^{14}C]-2-deoxy-D-glucose (specific activity 266 mCi/mmol) and [U-^{14}C]-glucose (specific activity 289 mCi/mmol) were from Perkin Elmer (Waltham,MA). All other chemicals were obtained from Sigma (Milano, Italy), unless otherwise stated.

The following antibodies were used for protein detection in Western blot: mouse monoclonal antibodies against LANCL2 [Vigliarolo T et al, 2015], UCP1 (Sigma), PPARγ 1/2 (Santa Cruz Biotechnology, Dallas, TX), vinculin (kindly provided by Prof. Emilia Turco, University of Turin, Italy), a rabbit polyclonal anti-GLUT4 (Abcam, Cambridge, UK), a rabbit polyclonal anti-pAkt (Santa Cruz Biotechnology) and a rabbit polyclonal anti-Akt (Cell Signaling Technology, Danvers, MA). Human adipose tissue (obtained from abdominoplasty performed on healthy subjects for esthetic reasons) was kept in complete DMEM medium during transportation from the surgical room to the laboratory and then immediately used for experiments. CD1 mice were purchased from Charles River Laboratories Italia (Calco, LC, Italy).

3.2. Cell culture and adipocyte differentiation

3T3-L1 mouse fibroblasts were purchased from LGC Standards and maintained in DMEM with 10% fetal calf serum (FCS) and penicillin/streptomycin in a humidified atmosphere containing 5% CO_2 at 37°C. For some experiments we used the same cell line 3T3-L1 kindly provided by Prof. Beguinot (University of Naples). For adipocyte differentiation, cells were seeded at 10^5 per well in 12-well plates or at 10^6 per 75 cm^2 flasks; at 2-day post confluence, adipogenesis was induced with a differentiation cocktail containing 100 nM insulin, 1 µM dexametasone, and 500 µM 3-isobuthyl-1-methylxanthine (IBMX) in DMEM with 10% FCS for 3 days, followed by 100 nM insulin in DMEM with 10% FCS for 5 days, changing the medium every 2–3 days. At day 8, the medium was switched to DMEM with 10% FCS without any addition for further 2 days before performing experiments: at day 5, approximately 60% of cells showed an adipocyte morphology, with accumulation of lipid droplets, while at day 10 this percentage increased to about 80-90%. During differentiation, 3T3-L1 cells were treated or not with 100 nM ABA. Adipogenic differentiation was monitored at day 1, 3 and 8 by q-PCR analysis of the specific adipogenic differentiation markers adiponectin, AP2, fatty acid synthase (FAS), GLUT4, PPARγ1 and 2 (PPARγ 1/2) and leptin, and at day 10 by lipid staining with Oil Red O Stain [Ariemma F et al, 2016]. Areas and diameters of fully differentiated adipocytes were measured using the Image J program; the measures were carried out on at least 150 cells for each condition.

AT-derived human mesenchymal stem cells (ATMSC) were purchased from Lonza (Basel, Switzerland) and cultured as described [Scarfi S et al, 2008]. Alternatively, they were purified from subcutaneous AT samples obtained from healthy subjects undergoing plastic surgery and cultured as described [Zuk PA et al,2011]. For adipogenic differentiation, ATMSC at the second passage were trypsinized and plated

onto 6-well plates at a density of $2x10^5$ cells/well. Cells were then cultured in a differentiation cocktail containing DMEM-F12 with 10% FCS and 100 nM insulin, 1 μM dexamethasone, 100 μM indomethacin and 500 μM IBMX, in the presence or absence of 100 nM ABA, and the medium was replaced every three days. Adipogenic differentiation was assessed at day 3, 7, 10 by q-PCR analysis of the specific adipogenic differentiation markers adiponectin, AP2, FAS, PPARγ and LPL. At day 10, 80-90% of cells showed accumulation of lipid droplets, as determined by Oil Red O staining [Ariemma F et al, 2016]. The browning effect of ABA was monitored at day 2, 5 and 8 by analysing the expression of the browning-specific markers, UCP1, PPARγ coactivator-1α (PCG-1α), cell death-inducing DNA fragmentation factor (CIDE-A), transmembrane protein 26 (TMEM26) and PRDM16.

3.3. Glucose uptake assay

Differentiated 3T3-L1 adipocytes, transfected or not with pcDNA6.2/V5/GW/D-TOPO© (empty, control plasmid) or with LANCL2-pcDNA6.2/V5/GW/D-TOPO© (LANCL2 plasmid), cultured in 12-well plates, were starved for 4 h in serum-free medium. Cells were then washed once with 1 ml of Krebs-Ringer HEPES buffer (KRH) and stimulated with 100 nM insulin or ABA in KRH for 1 h at 37°C. Glucose transport was measured by the addition of 0.5 mM D-glucose containing [^{14}C]-2-deoxy-D-glucose (0.5 μCi/well) for 20 min at 37°C. Glucose uptake was stopped by removal of the labeling mix and washing the cells 3 times with ice-cold KRH. Cells were then lysed with 0.05 M NaOH and radioactivity in each lysate was determined by scintillation counting in a Beta-Counter LS 6500 (Beckman-Coulter, Krefeld, Germany). Unspecific radioactivity uptake, determined in the presence of 20 μM cytochalasin B and 200 μM phloretin, was subtracted from each experimental value. For the experiment with the

PI3K inhibitor, cells were pre-incubated in the presence of 25 µM LY294002 for 30 min before the glucose uptake assay.

3.4. Evaluation of adipocyte oxygen consumption

3T3-L1 cells were cultured in the differentiation cocktail for 7 days with or without (control) 100 nM ABA, or were differentiated for 7 days and then incubated in complete DMEM for 24 h in the presence or absence of 100 nM ABA. At the end of differentiation process, cells were trypsinized and resuspended at 10^6 cells/ml in Hank's balanced salt solution (HBSS). Oxygen consumption was measured in a micro-respiratory system (Unisense A/S, Denmark). Cells were resuspended at 10^6/ml in HBBS and incubated at 37°C under stirring in a 300 µl-closed chamber, equipped with an oxygen micro-amperometric electrode; the linear rate of oxygen consumption was measured for 10 min. Protein concentration in the cell suspension was measured according to Bradford [Bradford MM, 1976].

3.5. Metabolic measurements in adipocytes

3.5.1. Triglyceride quantification

3T3-L1 cells were induced to differentiate as described above, in the presence or not of 100 nM ABA; triglycerides were measured at the end of differentiation (day 10). Triglycerides were also quantified in 3T3-L1 cultured in DMEM with 10% FCS, in the absence of the differentiating cocktail, with or without 100 nM ABA, and in 3T3-L1 differentiated in the absence of ABA and then incubated or not with 100 nM ABA for 24 h at the end of differentiation (day 10). Triglycerides were quantified using

AdipoSIGHT™ Triglyceride Assay kit (ZenBio, Research Triangle Park, NC), following the manufacturer's instructions.

3.5.2. Measurement of CO_2 production

3T3-L1 cells were induced to differentiate as described above and used at day 10. Cells were detached with trypsin and suspended in HBSS at 1.3×10^6 cells/ml. Then, 0.5 ml of this suspension was introduced in one of the two 3-ml chambers of a sealed glass vial especially designed for radioactive CO_2 quantification, while in the other chamber, connected to the first through a short channel allowing air exchange, 0.2 ml of 2 M NaOH was introduced to capture the radioactive CO_2 released by the cells (see Fig. 20C). [U-^{14}C]-D-glucose (0.5 mCi, final specific activity: 0.18 mCi/mmol), was added to the cell suspension, with or without 100 nM ABA or insulin, the vessel was tightly sealed and incubated at 37°C for 7 h. At the end of the incubation, the NaOH solution was counted in a Beta-Counter LS 6500 (Beckman-Coulter). The cell suspension was also withdrawn, washed once with 15 ml ice-cold HBSS, centrifuged at 2,000 *g* for 5 min at 4°C, and the cell pellet was lysed in 0.5 ml ice-cold deionized water. The cell lysate was then immediately subjected to lipid extraction as described in the following paragraph and an aliquot of the extract was used for scintillation counting.

3.5.3. Radioactive lipid synthesis/accumulation during differentiation

3T3-L1 cells were seeded at 2×10^5 cells/well in 6-well plates and cultured to confluence. Adipogenesis was then induced with the differentiation cocktail described above (insulin/dexametasone/IBMX) for 3 days, followed by 100 nM insulin for 3 days. After 6 days, the wells were washed once with HBSS and incubated for 5 h with 0.5 mCi of [U-^{14}C]-D-glucose (final specific activity: 0.09 mCi/mmol) in 1 ml HBSS

at 37°C in the presence of 100 nM insulin, with or without 100 nM ABA. At the end of the incubation, 1 ml of complete medium, without (control) or with 100 nM ABA or 100 nM insulin was added to each well, without removing the radioactive solution, and cells were further cultured for 4 days. Finally, cells were washed twice with ice-cold HBSS to remove free [^{14}C]-D-glucose and lysed in the wells with 0.5 ml of ice-cold deionized water. Cell lysates were withdrawn and immediately subjected to lipid extraction. Ten volumes of methanol followed by 10 volumes of chloroform were added to the cell lysates and incubated at 25°C for 20 min under gentle shaking. The solution was then centrifuged at 3,000 *g* for 10 min to remove precipitated proteins, the supernatant was further supplemented with 10 volumes of chloroform followed by 6 volumes of 50 mM KCl and vigorously shaken. The solution was then stored at -20°C overnight to allow phase separation. An aliquot of the organic phase from each sample was then withdrawn and used for scintillation counting. Experiments were performed in triplicate and repeated 4 times.

3.5.4 Glyceraldeyde-3-phosphate dehydrogenase (GAPDH) activity

Ten days after induction of differentiation, 3T3-L1 cells were washed twice with ice cold PBS, harvested in ice-coldHES buffer (20 mM Hepes, pH 7.4, 1 mM EDTA, 250 mM sucrose and protease inhibitors) and lysed by brief sonication. The lysates were centrifuged at 10,000 *g* for 10 min at 4°C. The supernatants were assayed for GAPDH activity at 23°C by measuring the reduction of NAD^+ in the presence of D-glyceraldehyde-3-phosphate, pyrophosphate buffer and disodium arsenate [Allison, WS et al, 1964].

3.6. LANCL2 silencing and overexpression

Transient transfection of 3T3-L1-derived differentiated adipocytes with LANCL2-specific siRNAs was performed at day 10 of differentiation using the Nucleofector System (Amaxa GmbH, Cologne,Germany). Adipocytes ($2.5x10^6$ cells) were transfected using the A033 program and the L Kit, with 2.5 μM LANCL2-targeting siRNA (siRNAL2, Oligo ID: SASI_Mn01_00042365) or with Mission Negative Control (Control, CTRL), obtained from Sigma. After transfection, cells were resuspended in DMEM supplemented with 10% FCS, penicillin (50 U/ml), and streptomycin (50 μg/ml), plated in 12-well plates (350.000/well) and incubated for 48 h in 5% CO_2 at 37°C. For LANCL2 overexpression, adipocytes at day 10 of differentiation were transfected with pcDNA6.2/V5/GW/D-TOPO© (empty, control plasmid) or with LANCL2-pcDNA6.2/V5/GW/D-TOPO©[Sturla L et al, 2009] using the Lipofectamine 2000 Reagent, following the manufacter's instructions. Glucose uptake experiments and gene expression assays were performed 48 h after transfection.

3.7. qPCR analyses

RNA extraction from 3T3-L1 cells was performed using the RNeasy Micro Kit (Qiagen, Milan, Italy). RNA extraction from adipose tissue was performed using QIAzol Lysis Reagent and TissueLyser instrument (Qiagen); the homogenates were extracted with chloroform and then RNA was purified using RNeasy Mini Kit (Qiagen) and quantified using a NanoDrop spectrophotometer (Nanodrop Technologies, Wilmington, DE). The cDNA was synthesized by using iScript cDNA Synthesis Kit (Bio-Rad Laboratories, Milan, Italy) starting from 1 μg of total RNA. PCR primers were designed through Beacon Designer 2.0 Software (Bio-Rad Laboratories) and are listed in Table I (mouse genes) and II (human genes).

Table I. PCR primers for mouse genes

Target Mouse gene	Accession number	Sequence, 5'-3'
PPARγ 1/2	NM_001127330 NM_011146	Forward 5'-GGAATTAGATGACAGTGACTTGGC-3' Reverse 5'-GGAGCACCTTGGCGAACAG-3'
GLUT4	NM_009204	Forward 5'-CCAGCCTACCGCCACCATAG-3' Reverse 5'-TTCCAGCAGCAGCAGAGC-3'
ADIPO-NECTIN	NM_009605	Forward 5'-GCTCTCCTGTTCCTCTTAATCC-3' Reverse 5'-GCAATCTCTGCCATCACG-3'
LEPTIN	NM_008493	Forward 5'-TGGCAGTCTATCAACAGGTC-3' Reverse 5'-GTGGAGTAGAGTGAGGCTTC-3'
Fatty Acid binding protein (AP2)	NM_024406	Forward 5'-AACACCGAGATTTCCTTCAAACTG-3' Reverse 5'-TCACGCCTTTCATAACACATTCC-3'
Fatty Acid Synthase (FAS)	NM_007988	Forward 5'-ATGGGTGTGGAAGTTCGTCAG-3' Reverse 5'-AGTGTGCTCAGGTTCAGTTGG-3'
UCP1	NM_009463	Forward 5'-GGAGGTGTGGCAGTGTTCAT-3' Reverse 5'-AAGCATTGTAGGTCCCCGTG-3'
PCG-1α	BC066868	Forward 5'-CCCTGCCATTGTTAAGACC-3' Reverse 5'-TGCTGCTGTTCCTGTTTTC-3'
Cidea	NM_007702	Forward 5'-TGCTCTTCTGTATCGCCCAGT-3' Reverse 5'-GCCGTGTTAAGGAATCTGCTG-3'
Tmem26	NM_177794	Forward 5'-TTCCTGTTGCATTCCCTGGTC-3' Reverse 5'-GCCGGAGAAAGCCATTTGT-3'
PRDM16	NM_027504	Forward 5'-GATGGGAGATGCTGACGGAT-3' Reverse 5'-TGTCTGACACATGGCGAGG-3'
TBX1	NM_011532	Forward 5'-CGAATGTTCCCCACGTTCCA-3' Reverse 5'-GTCTACTCGGCCAGGTGTAG-3'

FGF12	NM_020013	Forward 5’-CGTCTGCCTCAGAAGGACTC-3’ Reverse 5’-TCTACCATGCTCAGGGGGTC-3’
Mitochon-drial DNA	AP014941	Forward 5’-CCGTCACCCTCCTCAAATTA-3’ Reverse 5’-GGGCTAGGATTAGTTCAGAGTG-3’
UBIQUI-TIN	NM_019639	Forward 5’-GACAGGCAAGACCATCAC-3’ Reverse 5’-TCTGAGGCGAAGGACTAAG-3’
β-2 MICRO-GLOBULIN	NM_009735	Forward 5’-CGGTCGCTTCAGTCGTCAG-3’ Reverse 5’-CAGTTCAGTATGTTCGGCTTCC-3’

Table II. PCR primers for human genes

Target gene	Accession number	Sequence, 5'-3'
PPARγ 1/2	NM_138712 NM_015869	Forward 5'-CGAAGACATTCCATTCACAAG-3' Reverse 5'-CTCCACAGACACGACATTC-3'
GLUT4	NM_001042	Forward 5'-AATGCTGCTGCCTCCTATG-3' Reverse 5'-ATCAGAATGCCGATAACAATGG-3'
ADIPONECTIN	NM_001177800	Forward 5'-GCCTACCACATCACAGTC-3' Reverse 5'-TCAGCATAGAGTCCATTACG-3'
AP2	NM_001442	Forward 5'-AAGTCAAGAGCACCATAACC-3' Reverse 5'-TCAATGCGAACTTCAGTCC-3'
FAS	NM_004104	Forward 5'-TGTGGTCTTCTCCTCTGTG-3' Reverse 5'-TTGGTGCTCATCGTCTCC-3'
Lipoprotein Lipase (LPL)	NM_000237	Forward 5'- AGAGAGAACCAGACTCCAATG-3' Reverse 5'-GGCTCCAAGGCTGTATCC-3'
ACTIN	XM_005249818	Forward 5'-AATGAGCTGCGTGTGGCTCC-3' Reverse 5'-CAATGGTGATGACCTGCCG-3'
HPRT1	NM_000194	Forward 5'-GGTCAGGCAGTATAATCCAAAG-3' Reverse 5'-TTCATTATAGTCAAGGGCATATCC-3'

Quantitative real-time PCR (qPCR) was performed in an iQ5 real-time PCR detection system (Bio-Rad Laboratories) using 2× iQ Custom Sybr Green Supermix (Bio-Rad Laboratories). Values were normalized on mRNA expression of murine ubiquitin and β-2 microglobulin (reference genes for 3T3-L1) or of human β-actin and HPRT (for ATMSC). Statistical analysis of the qPCR was performed using the iQ5 Optical System Software version 1.0 (Bio-Rad Laboratories) based on the $^{2-}\Delta\Delta$Ct method [Livak KJ et

al, 2001]. The dissociation curve for each amplification was analysed to confirm absence of unspecific PCR products.

3.8. Western Blot

LANCL2, PPARγ 1/2, GLUT4, pAkt, Akt and UCP1 protein expression was determined by Western blot, using standard procedures. 3T3-L1 adipocytes differentiated in the presence or absence of 100 nM ABA and 3T3-L1 adipocytes, trasfected in parallel with pcDNA6.2/V5/GW/D-TOPO© (empty, control plasmid) and with LANCL2-pcDNA6.2/V5/GW/D-TOPO© (LANCL2 plasmid), incubated for 24 hours at 37°C in the presence or absence of 100 nM ABA, were washed three times with ice-cold HES buffer. Next, cells were collected by scraping in HES buffer containing a protease inhibitor cocktail for mammalian cells (Sigma) and homogenized by passing them through a 22-gauge needle for 10 times. All subsequent steps were performed at 4°C. The homogenate was centrifuged at 16,000 *g* for 30 min and the resulting pellet, enriched in cell membranes, was resuspended in Radioimmuno precipitation assay (RIPA) buffer (20 mM Tris-HCl pH 7.6, 150 mM NaCl, 1 mM EDTA, 1% NP40, 1% sodium deoxycholate, 0.1% SDS). Total protein content in the homogenate's pellet and supernatant was measured by a DC Protein Assay (Bio-Rad Laboratories). The same protocol was used for detection of pAkt and Akt in 3T3-L1 adipocytes transfected in parallel with negative control siRNA (CTRL) and with LANCL2-specific siRNAs (siRNA LANCL2); after 48 h from transfection, cells were starved for 4 h in serum-free medium and incubated for 30 min at 37°C with or without of 100 nM insulin, then collected and lysed as described before. SDS-PAGE was performed as mentioned in I chapter paragraph 3.1.6.

3.10. Statistical analysis

Experimental values are expressed as mean ± standard deviation of at least three independent experiments. All parameters were tested by *t* test for paired or unpaired data as appropriate. Values of $p<0.05$ were considered statistically significant.

4.0 Results

4.1. ABA stimulates GLUT4 expression and glucose uptake in differentiated murine adipocytes via a phosphatidyl inositol 3-kinase (PI3K)-dependent pathway

Treatment with ABA was previously shown to increase the plasmamembrane translocation of GLUT4 in murine adipocytes and to induce the concomitant phosphorylation of Akt [Bruzzone S et al, 2012 (a]. Here, we observed a significantly higher GLUT4 protein expression in membrane-enriched lysates from 3T3-L1-derived adipocytes differentiated for 5 days in an insulin-containing differentiation cocktail in the presence of 100 nM ABA compared to control cells, differentiated with the same cocktail but without the addition of ABA (Fig. 16A). The higher GLUT4 expression level in the ABA-treated adipocytes was paralleled by an approximately 2-fold increase of glucose uptake relative to adipocytes differentiated in the absence of added ABA (Fig. 16B). By comparison, insulin at the same concentration as ABA (100 nM) induced an approximately 3-fold increase of glucose uptake compared with untreated controls (Fig. 16B). Pre-treatment of adipocytes with the specific inhibitor of PI3K, LY294002, prior to incubation with [^{14}C]-2-deoxy-D-glucose, significantly reduced the stimulatory effect of both ABA and insulin on glucose uptake. This result, together with the previously observed ABA-induced phosphorylation of Akt in murine adipocytes [Bruzzone S et al, 2012 (a], suggests that ABA, similarly to insulin, activates glucose transport *via* a PI3K/Akt-dependent signaling pathway in adipocytes.

4.2. ABA increases O_2 consumption in 3T3-L1 adipocytes.

The effect of ABA treatment on the respiration of 3T3-L1-derived adipocytes was investigated in two different experimental settings: cells were either differentiated for 7 days with the standard differentiation cocktail, containing or not 100 nM ABA, or cells were first differentiated for the same time in the absence of ABA, and then treated or not with the hormone for 24 h in the absence of the differentiation cocktail.

As shown in Fig. 17A, adipocytes differentiated in the presence of 100 nM ABA showed a significantly increased respiration compared with untreated controls (28 ± 4 vs. 22 ± 2 nmol O_2/min/mg protein, respectively); a similar increase of O_2 consumption (29 ± 4 vs. 21 ± 3 nmol O_2/min/mg protein in ABA-treated vs. control cells) was also observed when adipocytes were exposed to ABA for 24 h only, after being differentiated for 7 days in the absence of the hormone (Fig. 17B).

4.3. LANCL2 silencing abrogates, and LANCL2 overexpression enhances, the stimulation of glucose uptake induced by ABA and insulin in adipocytes

LANCL2 has been identified as the ABA receptor in mammalian cells [Sturla et al, 2009 and 2011]. To investigate whether LANCL2 expression modulates glucose uptake in adipocytes, 3T3-L1-derived adipocytes were first transfected with a LANCL2-targeting siRNA (siRNA LANCL2) or with a negative control siRNA (Control, CTRL). At 48 h after transfection, a 45% decrease of LANCL2 expression was obtained (Fig. 18A); on these cells, we explored whether LANCL2 silencing had a direct effect on glucose uptake, by measuring ABA- or insulin-dependent glucose transport. LANCL2 silencing abrogated the increase of glucose uptake induced by both ABA and insulin (Fig. 18B) and also significantly reduced insulin-stimulated Akt phosphorylation and GLUT4 protein expression (Fig. 18C).

To confirm a role for LANCL2 expression levels on adipocyte glucose uptake, parallel experiments were performed where LANCL2 was overexpressed. 3T3-L1-derived adipocytes were transfected with pcDNA6.2/V5/GW/D-TOPO© (empty plasmid, used as a control) or with LANCL2-pcDNA6.2/V5/GW/D-TOPO© (LANCL2 plasmid). Overexpression of the LANCL2 protein was confirmed by Western blot analysis 48 h after transfection (Fig. 19A). At the same time point, differentiated 3T3-L1 adipocytes, overexpressing or not LANCL2 protein, were treated with either 100 nM ABA or insulin for 1 h and glucose uptake was then measured. Basal (unstimulated) glucose transport was significantly enhanced in LANCL2-overexpressing cells compared with controls (approximately 3-fold) and incubation for 1 h with ABA or insulin (both at 100 nM) further increased glucose transport significantly, by approximately 60% for both hormones (Fig. 19A). The expression levels of GLUT4 and of PPARγ were also investigated in differentiated 3T3-L1 adipocytes overexpressing LANCL2. As revealed by qPCR analysis, GLUT4 and PPARγ mRNA levels were higher in LANCL2-transfected cells relative to controls (showing an approximately 3- and 1.5-fold increase, respectively, Fig. 19B, C), and also the corresponding protein levels were similarly increased, as detected by Western blot (insets in Fig. 19B and C). In addition, incubation of LANCL2-overexpressing cells with 100 nM ABA or insulin further increased the expression levels of GLUT4 and PPARγ mRNAs and proteins, as compared with control cells (Fig. 19B, C, D).

These results demonstrate that the level of LANCL2 expression in adipocytes affects both basal and ABA or insulin-stimulated glucose uptake *via* GLUT4, as well as expression of GLUT4 and PPARγ, the master regulator of adipogenesis.

4.4. Metabolic effects of ABA on differentiated 3T3-L1 adipocytes

At two-days post confluence, 3T3-L1 preadipocytes were induced to differentiate with a cocktail containing insulin, dexametasone and IBMX (see Materials and Methods) for 10 days in the absence (control) or in the presence of 100 nM ABA. Upon staining of accumulated lipids with Oil Red O, the ABA-treated adipocytes appeared smaller in size compared with the untreated controls (Fig. 20A, right panel). Thus, the cell surface area and diameter were measured on stained cells and the results confirmed that ABA treatment during differentiation resulted in a smaller size of the adipocytes (Fig. 20A, left panel): cell area and diameter in ABA-treated adipocytes were 37% and 21% smaller, respectively, compared with control cells.

In the absence of the differentiation cocktail, ABA *per se* was unable to induce the differentiation of 3T3-L1 pre-adipocytes: incubation of the cells for up to 10 days in the presence of ABA alone (Fig. 20B, black bars), at concentrations up to 10 µM (bar 2), did not induce any accumulation of triglycerides (see bar 1 for comparison). When 100 nM ABA was added to the insulin/dexametasone/IBMX cocktail during differentiation (Fig. 20B, white bars), the triglyceride content at 10 days-post induction of differentiation, expressed as mMol/mg protein, was slightly lower in the ABA-treated adipocytes (bar 4) compared with control, ABA-untreated cells (bar 3). We then measured the triglyceride content in 3T3-L1 adipocytes cultured for 10 days in the presence of the differentiating cocktail (pre-differentiated, grey bars), then washed, resuspended in complete medium without cocktail and incubated for 24 h without (bar 5) or with 100 nM ABA (bar 6) or insulin (bar 7) or 100 nM ABA + 100 nM insulin (bar 8): the amount of triglycerides was not modified in cells treated with ABA compared with untreated controls (bars 6 and 5, respectively); conversely, it was significantly increased in adipocytes incubated with 100 nM insulin (bar 7) compared

with controls (bar 5). Addition of 100 nM ABA to insulin did not further increase the triglyceride content of differentiated cells (bar 8).

The GAPDH activity was increased by approximately 50% in cells differentiated in the presence of ABA compared to untreated controls (not shown), suggesting an enhanced glucose metabolism through the glycolytic pathway in ABA-treated adipocytes.

Finally, the effect of ABA on CO_2 production, reflecting hexose monophosphate shunt and tricarboxylic acid cycle activities, and fatty acid synthesis from labeled glucose was compared with that of insulin on differentiated 3T3-L1 cells. CO_2 production by adipocytes treated with 100 nM ABA for 7 h was increased compared with untreated controls, although the increase was significantly lower compared with that observed with insulin at the same concentration (Fig. 20C, black bars). Fatty acid synthesis from labelled glucose was not modified in differentiated adipocytes incubated for 4 days with ABA compared with untreated controls, in contrast with the significant increase induced by insulin (Fig. 20C, striped bars). No additive effect was observed in cells treated with ABA and insulin, both at 100 nM, and no further increase of CO_2 release or lipid synthesis was observed at micromolar ABA concentrations (not shown).

Collectively, these data indicate that ABA, unlike insulin, does not *per se* induce adipocyte differentiation; when present during the insulin-induced adipocyte differentiation process, ABA appears to induce a remodeling of the cells, reducing cell size and triglyceride content. Like insulin, ABA stimulates glucose oxidative metabolism (CO_2 production), but lipid synthesis from glucose is less than that observed with insulin.

4.5. Transcriptional effects of ABA on 3T3-L1-derived adipocytes and on human ATMSC

To further evaluate the effect of ABA on gene transcription during adipocyte differentiation, both 3T3-L1 and ATMSC cells were induced to differentiate, by culture in the respective differentiation cocktails, in the presence or absence of 100 nM ABA: expression of the typical adipocyte markers was explored at days 1, 3 and 8 of the differentiation process in 3T3-L1 cells and at days 3, 7, 10 and 16 in ATMSC.

Adiponectin and leptin mRNAs were both significantly increased in ABA-treated 3T3-L1 derived adipocytes compared with untreated controls (2.9- and 2.5-fold, respectively) as early as 24 h after induction of differentiation (Fig. 21A), and this up-regulation persisted, although to a lower extent, also at day 3. Transcription of PPARγ, also increased, slightly but significantly, in ABA-treated cells, both at day 1 and at day 3 of differentiation (with a 15% and 26% increase relative to controls, respectively). Conversely, the fatty acid synthase (FAS) mRNA levels were slightly increased by the presence of ABA only at day 3 of differentiation. Finally, the transporters of free fatty acids (FFA) AP2 and of glucose (GLUT4), were up-regulated by ABA treatment as compared with control cells, showing a significant increase both at day 1 and 3, yet with different kinetics; these data are in agreement with the increased expression of GLUT4 shown in Fig. 16A. The expression levels of all genes explored were not further increased at the same time points when cells were incubated with 10 μM instead of 100 nM ABA.

In ATMSC differentiated in the presence of 100 nM ABA (Fig. 21B), we observed an increased expression of the adiponectin, FAS, and lipoprotein lipase (LPL) genes compared with untreated controls, which peaked at day 7 post-induction of differentiation; the PPARγ and GLUT4 mRNAs were increased at day 3 of differentiation (Fig. 21B). AP2 expression was significantly higher in ABA-treated

ATMSC compared with untreated controls at all time points explored. At 16 days post-induction of differentiation, the mRNA levels of all the genes explored in 3T3-L1 and in ATMSC were not significantly different in ABA-treated compared with control cells.

Finally, we tested the effect of ABA on the transcription of GAPDH, leptin, GLUT4, adiponectin and PPAR-γ in adipocytes terminally differentiated in the absence of ABA. When 3T3-L1-derived adipocytes and human adipose tissue obtained from abdominoplasty were exposed to 100 nM ABA, the mRNA level of all these genes was significantly increased over values observed in untreated cells after only 4 h incubation (Fig. 21C).

4.6. ABA induces brown features in 3T3-L1 adipocytes

Altogether, the results obtained from the metabolic studies indicated that ABA significantly stimulates glucose transport (Fig. 16B), O_2 consumption (Fig. 17) and CO_2 production (Fig. 20C) in adipocytes, with a lesser increase of lipid synthesis compared with insulin (Fig. 20B, C). We then investigated whether ABA could induce the activation of adipocyte genes regulating the "browning" process which would be coherent with the observed increased metabolic rate and reduced triglyceride accumulation. To this purpose, 3T3-L1 cells were treated during the differentiation process either without (control) or with ABA at two different concentrations (100 nM and 10 μM) and the mRNA levels of the brown adipocyte markers UCP1, PGC-1α, PRDM16, CIDE-A [Barneda, D et al, 2013] and TMEM26 were compared in ABA-treated and in control cells. mRNA levels from all genes explored were up-regulated in ABA-treated compared with control cells, at both concentrations tested and at all time points (day 2, 5 and 8 post-induction of differentiation), except for PRDM16, which increased over control values at days 5 and 8, but not at day 2 (Fig. 22). mRNA levels of UCP1 and PRDM16 progressively increased during exposure of the cells to

ABA, reaching 3-fold higher values relative to controls at day 8 (Fig. 22). The increased expression of UCP1 was confirmed by Western blot, showing an approximately 2- and 4-fold increase of the protein relative to control, in cells cultured for 8 days with 100 nM or 10 μM ABA, respectively (Fig. 22, inset to the first panel). When 100 nM ABA was added at the end of the differentiation process (day 10) for 24 h, a significant increase of mRNA levels of UCP1, PGC-1α, CIDE-A and FGF21 was observed relative to ABA-untreated cells (3.2 ± 0.5, 2 ± 0.1, 2.9 ± 0.2, 7.5 ± 0.9 respectively n=3).

5.0 Discussion

Altogether, these results suggest that ABA enhances glucose disposal in white adipocytes and induces brown fat activity in these cells.

Indeed, ABA increases protein expression of GLUT4 and stimulates glucose uptake in differentiated murine 3T3-L1 adipocytes (Fig. 16A and B). The underlying signaling pathway requires the ABA receptor LANCL2 (Fig. 18B and 19A), and also involves the activation of PI3K (Fig. 16B). ABA was already shown to induce the phosphorylation of Akt in murine adipocytes [Bruzzone S et al,2012 (a] and LANCL2 can promote maximal phosphorylation of Akt in liver cells in response to mitogenic signals by binding and activating the Akt kinase mTORC2 [Zeng M et al, 2014]. Altogether, these results indicate that ABA, via LANCL2, activates both PI3K and Akt in adipocytes.

Interestingly, even in the absence of added ABA, over-expression of LANCL2 significantly increases GLUT4 expression (Fig. 19B) and basal, as well as insulin-stimulated, glucose uptake in differentiated murine adipocytes (Fig. 19A). Conversely, silencing of LANCL2 abrogates not only the enhancing effect of ABA on glucose uptake, but also that of insulin; indeed, a 40% decrease of LANCL2 expression is sufficient to abrogate glucose uptake induced by insulin (Fig. 18B). These data suggest that, by modulating the level of GLUT4 expression, the ABA/LANCL2 system can impact on insulin action in adipocytes and thus on whole-body glycemia homeostasis. Indeed, ablation of GLUT4 in adipocytes results in systemic insulin resistance [Abel ED et al, 2001]. Conversely, an increased GLUT4 expression in adipocytes normalizes fasting hyperglycemia and glucose intolerance in mice lacking GLUT4 selectively in muscle [Carvalho E et al, 2005]. GLUT4 expression is regulated by PPARγ, whose activation mediates the anti-diabetic effects of thiazolidinediones (TZDs) [Arner P,

2003; Saltiel AR et al, 1996; Smith SA, 2003]. Treatment of patients with TZDs, such as rosiglitazone and pioglitazone, lowers plasma glucose levels and induces remodeling of the adipose tissue, whereby large adipocytes are replaced with small and/or insulin-sensitive cells [Okuno AJ et al, 1998; de Souza CJ et al, 2001]. Pointedly, ABA treatment reduces adipocyte diameter and area (Fig. 20A), suggesting that adipocyte remodeling may be one of the effects of ABA on AT. ABA was previously shown to activate PPARγ in 3T3-L1 pre-adipocytes *in vitro*, although it was significantly less potent than the synthetic agonist rosiglitazone [Guri AJ et al, 2007]. Here we observed that incubation with ABA or transfection with LANCL2 (Fig. 19C) increases mRNA levels and protein expression of PPARγ in differentiating murine and human adipocytes (Fig. 21A, B) and in already differentiated murine (Fig. 19C) and human adipocytes (Fig. 21C). Both PPARγ isoforms appear to be upregulated by ABA and LANCL2 overexpression (Fig. 19C). Upregulation of PPARγ expression *per se* is known to suppress GLUT4 transcription [Armoni MJ et al, 2003], unless PPARγ is bound to co-activators or to ligands (such as TZDs), causing its dissociation from the GLUT4 promoter. Thus, the increased transcription of the PPARγ activator PGC-1α induced by ABA (Fig. 21) may be responsible for the induction of GLUT4 transcription. Indeed, overexpressed PGC-1α has been shown to bind PPARγ and to increase GLUT4 expression and glucose transport in muscle cells [Michael LF et al, 2001].

The discovery that LANCL2 expression levels affect the sensitivity of adipocytes to insulin-stimulated glucose uptake and the recent demonstration of its non-canonical properties as a G protein-coupled receptor also capable of nuclear translocation [Fresia C et al, 2016] identify LANCL2 as a new target for investigations on the genetic background of adipocyte insulin resistance and for therapeutic interventions aimed at increasing adipocyte glucose uptake without increasing triglyceride deposition.

In contrast to insulin and TZD PPARγ agonists (e.g. rosiglitazone), ABA does not *per se* induce adipocyte differentiation, neither in murine pre-adipocytes nor in human ATMSC. Moreover, the amount of triglycerides in adipocytes incubated with ABA is significantly lower than that measured in cells treated with insulin (Fig. 20B, C) or rosiglitazone (not shown). The fact that ABA induces a more limited triglyceride accumulation in adipocytes compared to insulin and to TZDs may prove advantageous, if ABA supplementation were proposed for the treatment of glucose intolerance [Magnone M et al, 2015].

In vitro, ABA upregulates the expression of various adipocyte marker genes, such as AP2, adiponectin, FAS and leptin during the early phase of human and murine adipocyte differentiation (Fig. 21A, B); however, at the end of differentiation, the expression level of these genes in the ABA-treated cells is not different from that observed in the untreated controls, with the exception of AP2 mRNA in ATSMC (Fig. 21B). Thus, the effect of ABA on adipocyte differentiation appears to be one of acceleration rather than induction. Among the genes upregulated by ABA, adiponectin plays a crucial role in the prevention of diabetes mellitus and metabolic syndrome, as high adiponectin levels protect against the impairment of glucose metabolism [Koerner A et al, 2005; Maeda K, 2007]. Adiponectin has anti-diabetic, anti-inflammatory, anti-atherogenic and cardio-protective properties, and an increase of this adipokine could contribute to important clinical benefits in the development of therapies for the prevention or treatment of obesity and obesity-related diseases. Recently Hui et al described that adiponectin enhances cold-induced browning of subcutaneous adipose tissue and that adiponectin KO mice are resistant to subcutaneous adipose browning during cold adaptation [Hui X et al, 2015]. Our results indicate that ABA indeed stimulates browning of white adipocytes by increasing the expression levels of several key proteins involved in the browning

process including UCP1 (Fig. 22). UCP1 is the key marker of BAT and its expression is regulated by several transcriptional factors. Among them, C/EBPβ and PPARγ [Tontonoz P et al, 1994; Brun RP et al, 1997] are critical to initiate both white and brown adipogenesis, whereas PDRM16 and PPARγ coactivator-1α (PCG-1α) are essential to brown fat determination, by stimulating expression of brown-specific genes [Lee YH et al, 2014; Barbera MJ et al, 2001;Uldry M et al, 2006]. The increased expression of the beige cell marker TMEM26 [Wu J et al, 2012] and of the brown cell marker CIDE-A [Barneda D et al, 2013] in the ABA-treated adipocytes suggests that ABA may be able to convert white into beige/brown adipocytes. The observations that adipocytes differentiated in the presence of ABA have a reduced size compared with untreated cells (Fig. 20A), accumulate less triglycerides and synthesize significantly less fatty acids from glucose compared with insulin-treated cells (Fig. 20B, C) are in line with the hypothesis that glucose-derived energy conversion into lipid synthesis is less efficient in ABA- than in insulin-treated cells.

In conclusion, the fact that ABA stimulates glucose uptake and UCP-1 expression by BAT and induces expression of browning genes in WAT and in WAT-derived preadipocytes makes it an attractive hormonal therapy to improve glucose tolerance under conditions of insulin resistance and obesity.

CONCLUDING REMARKS AND PERSPECTIVES

Type 2 diabetes mellitus (T2DM) is already a worldwide health emergency and its prevalence is steadily increasing, making new therapeutic and preventive approaches an urgent need.

The results obtained in this thesis demonstrates that abscisic acid (ABA) is implicated in glycemic control through its receptor LANCL-2. Indeed, we demonstrate the role of ABA in the hormonal cross-talk between insulin and GLP-1, which lies at the heart of glycemia homeostasis. We observed a positive feedback mechanism between ABA and GLP-1, which is relevant to the physiology of glycemia regulation and may also be explored as a means to improve endogenous GLP-1 function in T2DM patients.

We further demonstrate that ABA stimulates glucose uptake and UCP-1 expression by brown adipose tissue and induces expression of browning genes in the WAT and in WAT-derived preadipocytes. Finally, we observed a protective role of ABA on hypoxia-induced neuronal cell death.

Altogether, these results suggest that dietary ABA may be considered as a new therapeutic intervention to control hyperglycemia, reduce WAT mass and improve neuroprotection in the diabetic or pre-diabetic subject.

These results provide a strong rationale for testing the possibility of exploiting ABA as a new anti-diabetic drug, possibly in combination with GLP-1 mimetics, in the clinical setting for the treatment of subjects with prediabetes, diabetes and the metabolic syndrome.

FIGURES

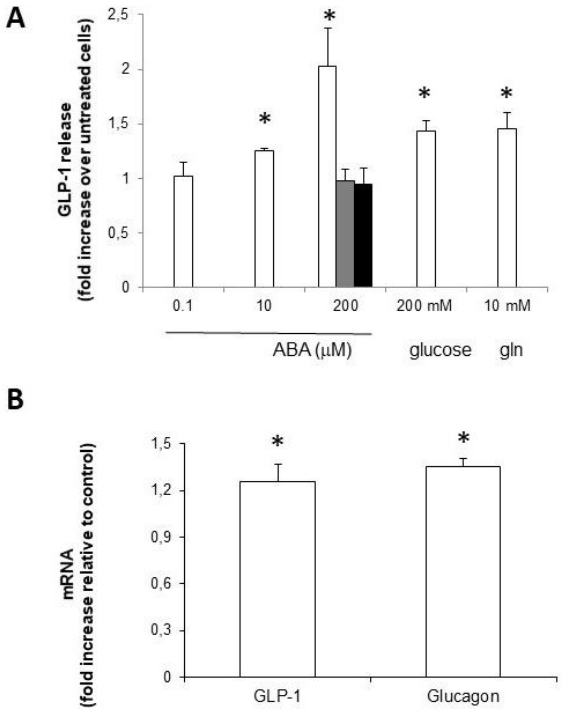

Fig. 6. ABA induces GLP-1 release and transcription in hNCI-H716 cells.

A. hNCI-H716 cells were incubated for 2 h in the absence or presence of ABA (at the indicated concentrations), or of 200 mM glucose or 10 mM glutamine (gln). In some experiments, cells were pre-incubated for 10 min in the absence or presence of 20 µM 2',3'-Dideoxyadenosine, a specific adenylyl cyclase inhibitor (grey bar) or of 1 µM of a cell permeable PKA inhibitor (protein kinase A inhibitor 14-22 amide, myristoylated, black bar), prior to stimulation with 200 µM ABA. GLP-1 levels in the culture media were then estimated with an ELISA kit. Data, expressed as fold increase over values in untreated cells, are expressed as mean ± SD of at least 3 different experiments. *$p<0.05$ compared to untreated cells. **B.** hNCI-H716 cells were incubated for 2 h in the absence or presence of 200 µM ABA and qPCR was performed with specific primers for GLP-1 and glucagon; *$p<0.05$ compared to expression in untreated cells.

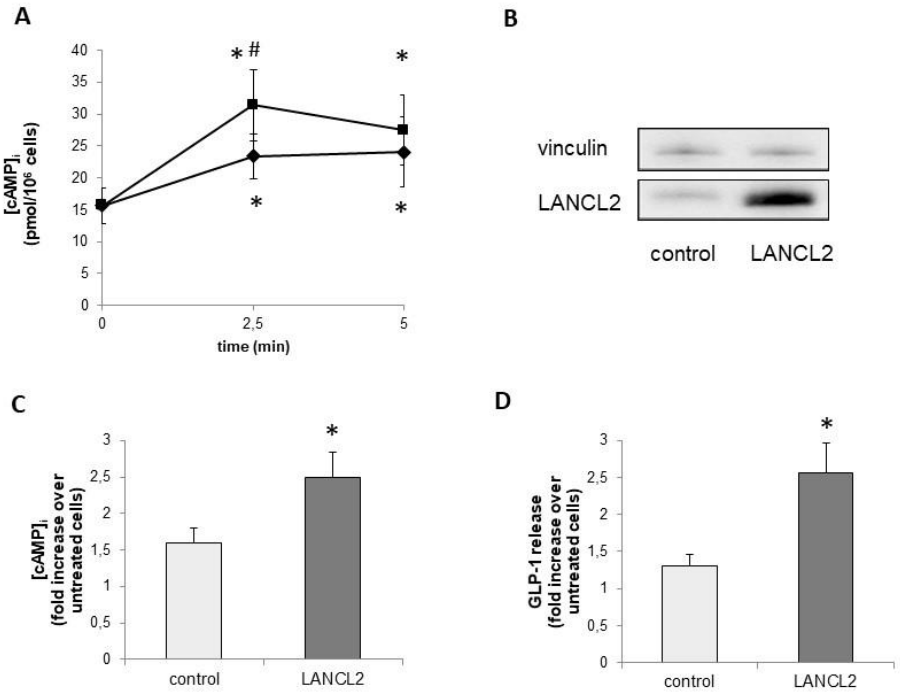

Fig. 7. ABA induces the increase of the $[cAMP]_i$ in hNCI-H716 cells

A. hNCI-H716 cells were incubated for the indicated time in the absence or presence of 200 µM ABA (squares), or of 10 mM glutamine (rhombi); $[cAMP]_i$ was then measured on cell extracts. Data are mean ± SD of at least 3 different experiments; *p<0.05 compared with untreated cells; #p<0.05 compared to glutamine-treated cells (for the same time). **B**. hNCI-H716 cells were transfected with an empty plasmid (control) or with a LANCL2-containing plasmid (LANCL2). After 48 h from transfection, cells were lysed and a Western blot analysis was performed using an anti-LANCL2 monoclonal antibody [Vigliarolo T et al, 2015]; a representative blot is shown, confirming LANCL2 overexpression after transfection. LANCL2 expression was normalized on vinculin levels. **C**. After 48 h from transfection, cells were stimulated for 2.5 min in the absence or presence of 200 µM ABA. $[cAMP]_i$ was measured on cell extracts and data, expressed as fold increase over values in unstimulated cells, are expressed as mean ± SD of at least 3 different experiments; basal cAMP values were not

significantly different upon transfection. *p<0.05 compared to control. **D.** After 48 h from transfection, cells were incubated for 2 h in the absence or presence of 200 μM ABA. GLP-1 levels in the culture media were then estimated with an ELISA kit. Data, expressed as fold increase over values in unstimulated cells, are expressed as mean ± SD of at least 3 different experiments. *p<0.05 compared to untreated cells.

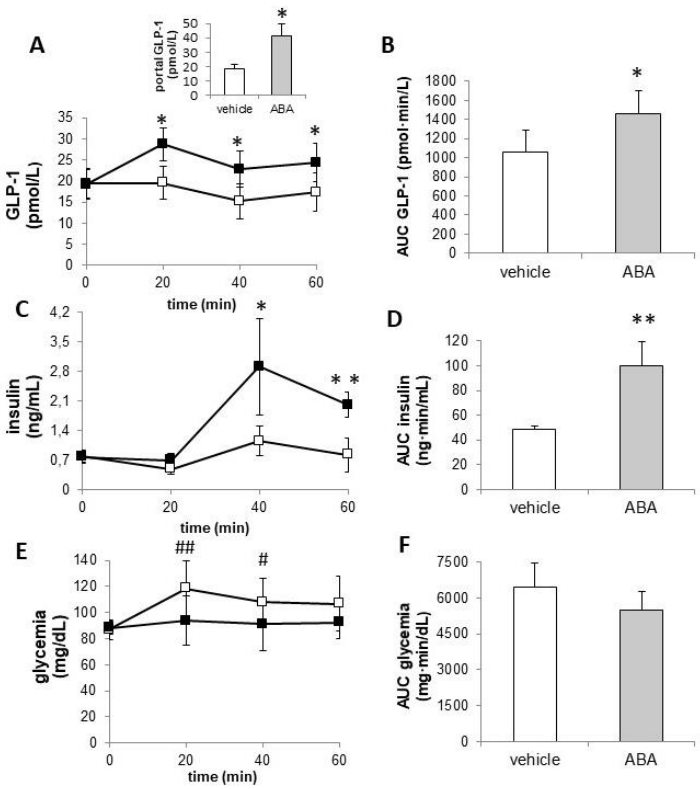

Fig. 8. Effect of oral ABA on plasma GLP-1, insulin and glucose levels in rats.

ABA (50 mg/Kg, black squares) or vehicle alone (open squares) were orally administered to rats pre-treated with Sitagliptin (6 animals per experimental group) and blood samples were collected at 0, 20, 40 and 60 min to evaluate plasma GLP-1 (**A**), insulin (**C**) and glucose (**E**). The AUC corresponding to the curves of GLP-1 (**B**), insulin (**D**) and glycemia (**F**) were calculated. Inset to panel A: blood samples were collected from the portal vein of rats not pre-treated with Sitagliptin, 10 min after ABA or vehicle administration and GLP-1 levels were evaluated (n=5 rats per group). *p<0.05 and **p<0.01 compared with the corresponding value in vehicle-treated animals; #p<0.05 and ##p<0.01 compared with time zero.

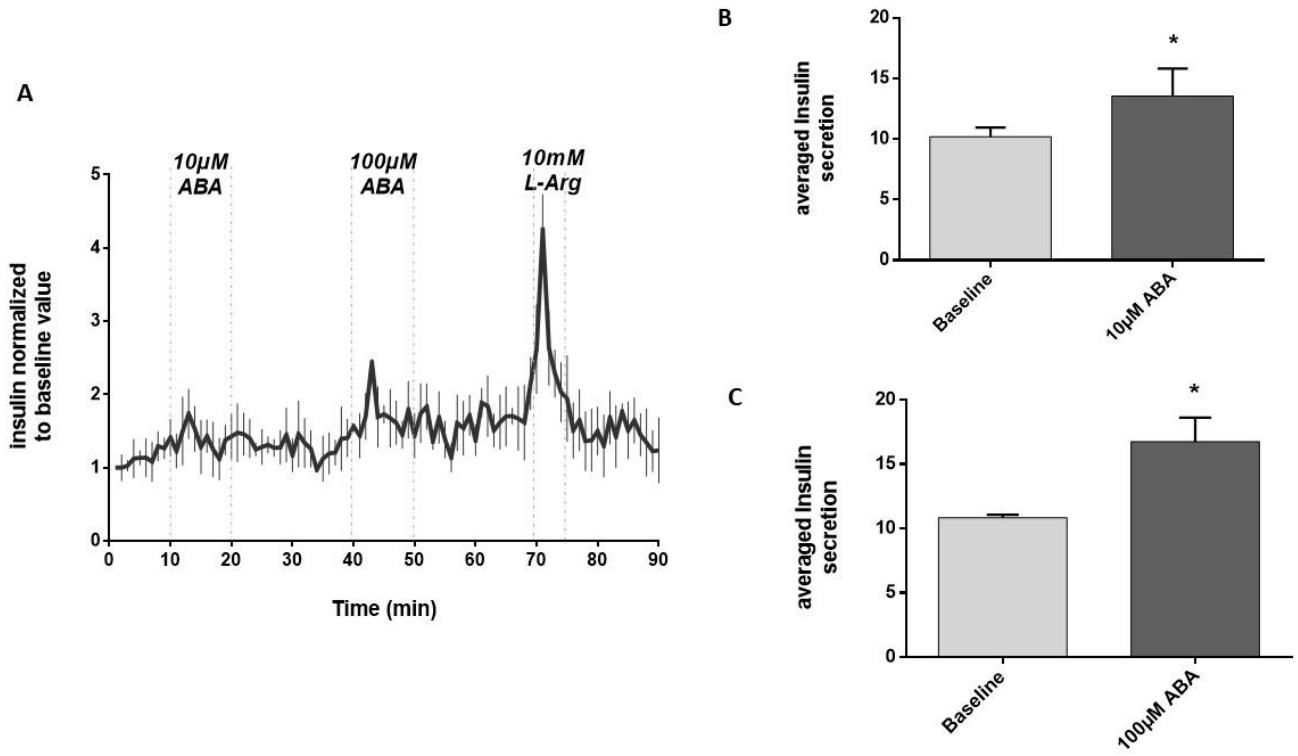

Fig. 9. ABA stimulates insulin release from perfused pancreas.

Rat pancreas were perfused for 10 min with 10 µM and 100 µM ABA in high glucose buffer (10 mmol/L glucose), when indicated. **A.** Insulin levels were normalized to the basal level in each trace. **B, C.** The area under the curve was calculated during the first 10 min (baseline) or during the 10 min infusion with ABA. Data are expressed as mean ± SD (n=5). Statistical analyses were calculated with the paired *t*-test: *p=0,05.

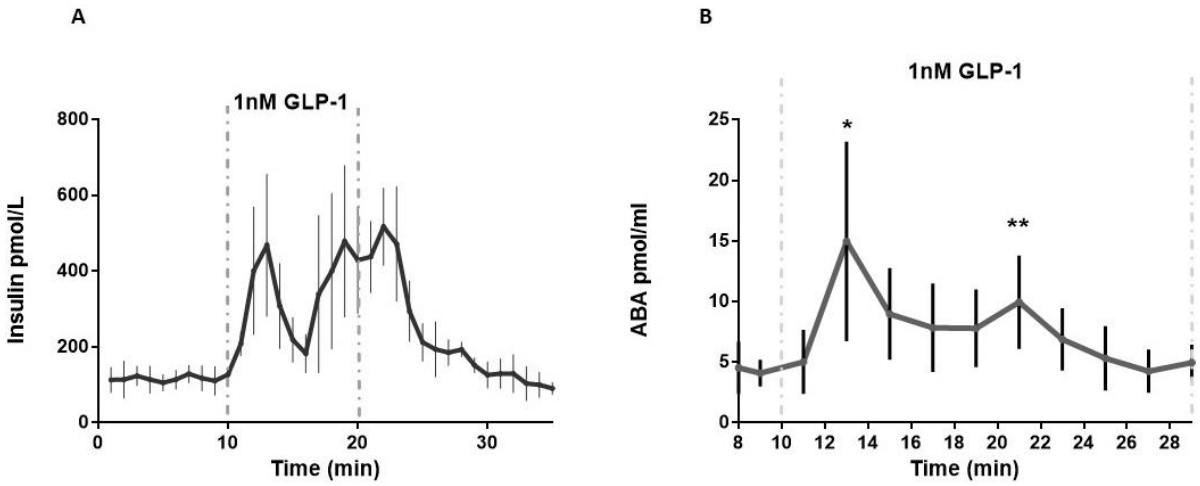

Fig. 10. GLP-1 stimulates the release of both insulin and ABA from pancreas.

Rat pancreas were perfused with 1 nM GLP-1 in high glucose buffer (7 mmol/L glucose). Insulin (**A**) and ABA (**B**) were measured in the effluent samples. Data are mean values ± SD (n=6). Statistical analysis was conducted by *t*-test:*p<0,018; **p< 0,027 compared to basal level at min 9, prior to GLP-1 infusion.

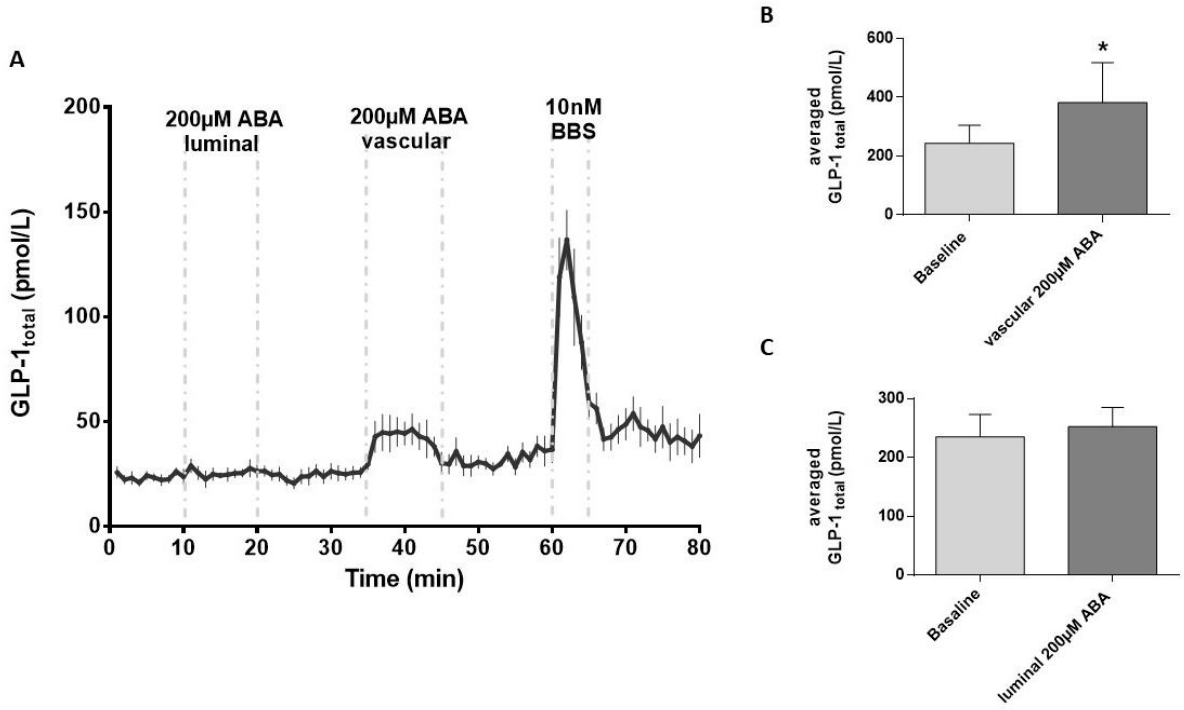

Fig. 11. Vascular, but not luminal, ABA stimulates GLP-1 secretion from perfused rat proximal small intestine.

Rat proximal small intestine were perfused with ABA, as indicated on the trace. **A**. Total GLP-1 levels were determined; data are shown as mean values ± SEM (n=5). **B,C** The area under the curve was calculated during the first 10 min (baseline) or during the 10 min perfusion with ABA. Data are shown as mean values ± SD. Statistical analyses were calculated by paired *t*-test; *p<0.048.

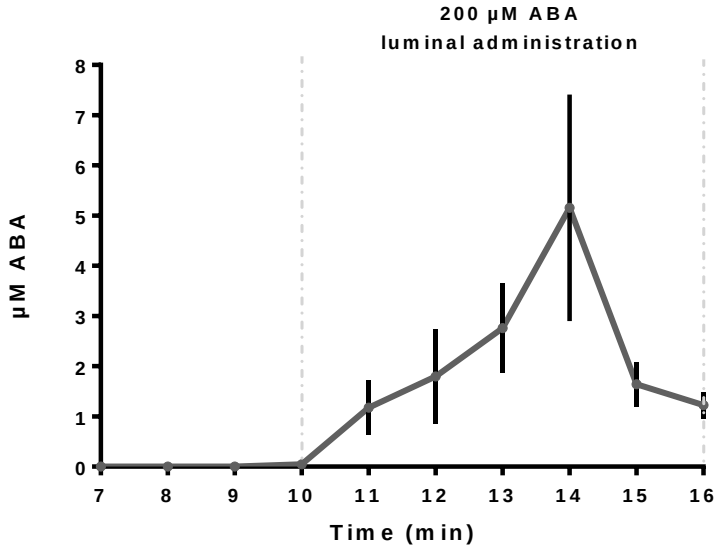

Fig. 12. Luminally administered ABA is absorbed by the intestine.

ABA (200 µM) was perfused in rat proximal small intestine. ABA levels in the venous effluent were determined. Data are shown as mean values ± SD (n=5). All points after 2 min of infusion were statistical significant compared to the baseline (9min).

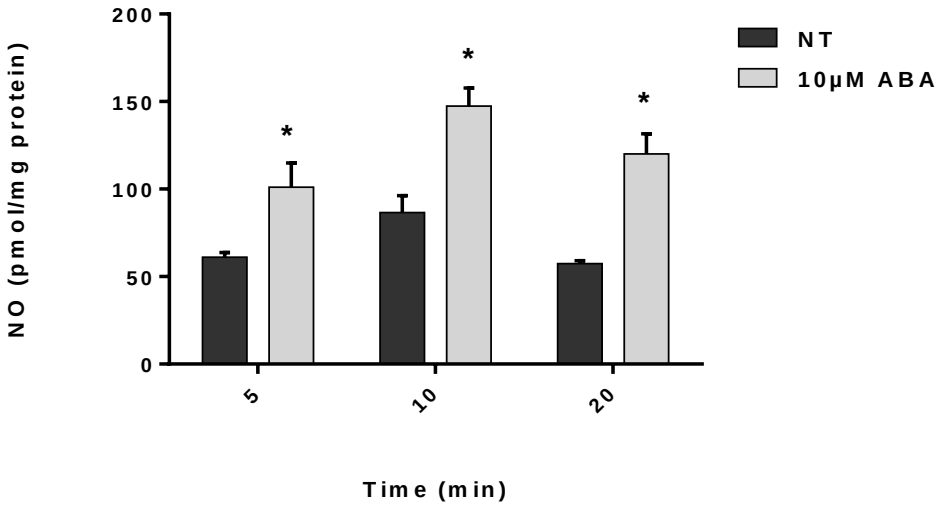

Fig. 13. ABA stimulates NO release by N2a cells.

N2a cells were stimulated (or not) with 10 µM ABA for 5, 10, 20 min of treatment and NO release was measured. Value are mean ± SD of 3 different determinations. *p<0,05.

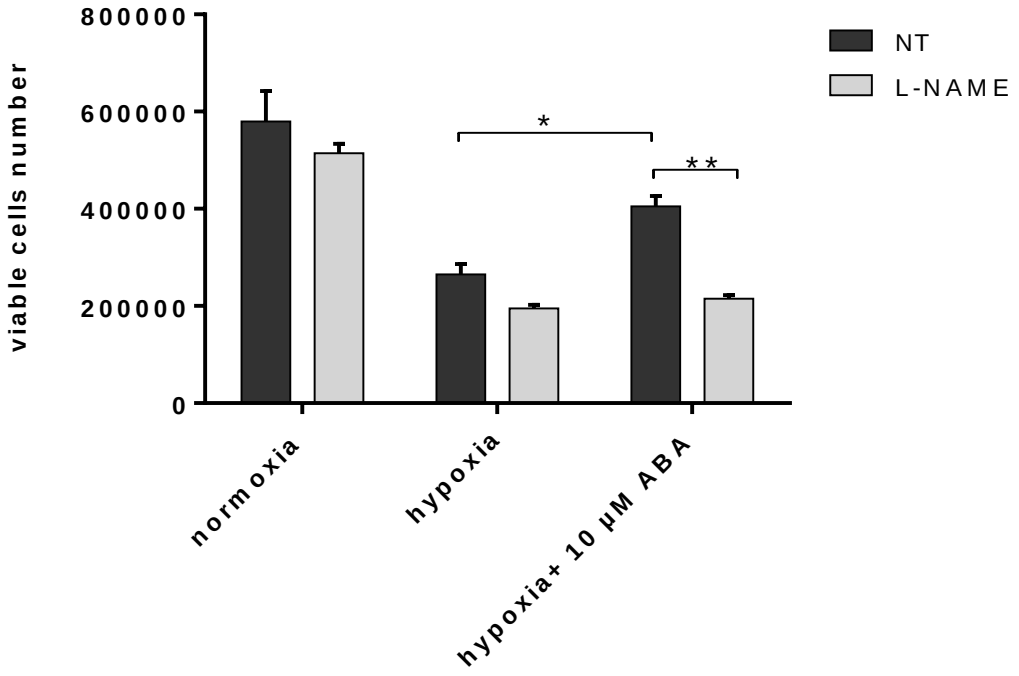

Fig. 14. ABA improves survival of N2a cells to hypoxia *via* NO.

Hypoxia conditions were created as described in the Materials and Methods section, in the presence or absence of 10 µM ABA, with or without L-NAME (as indicated). After 6h, cell mortality was evaluated by cell counting and Trypan blue exclusion. *p<0.02; **p<0.01. Results represent mean ± SD of 3 differentdeterminations.

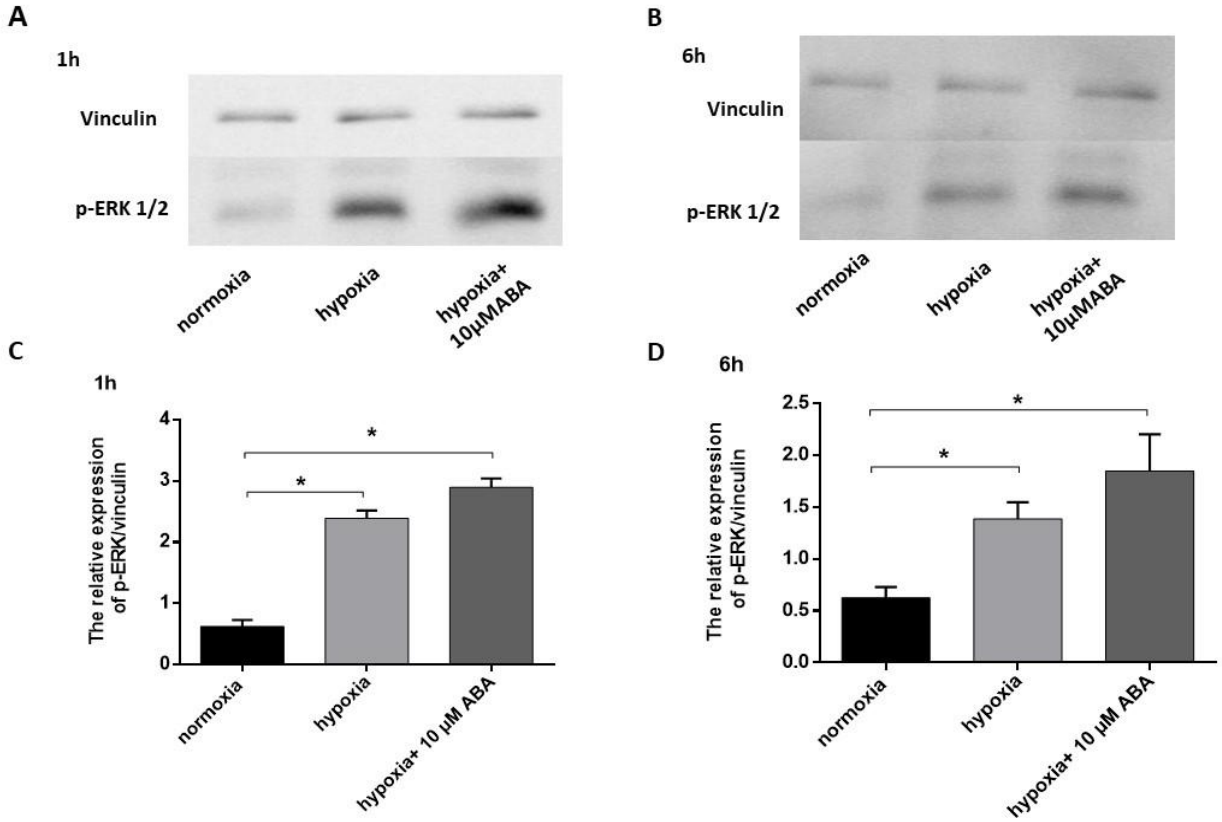

Fig. 15. ABA induces up-regulation of p-ERK in N2a cells under hypoxia.

Western blot analyses were performed to detect the levels of p-ERK. **A, B**. Protein expression was analysed after 1h and 6h of hypoxic stress. One representative result is shown. **C, D** Levels of p-ERK were normalized to vinculin levels (mean ± SD of 3 different determinations) *p<0,05

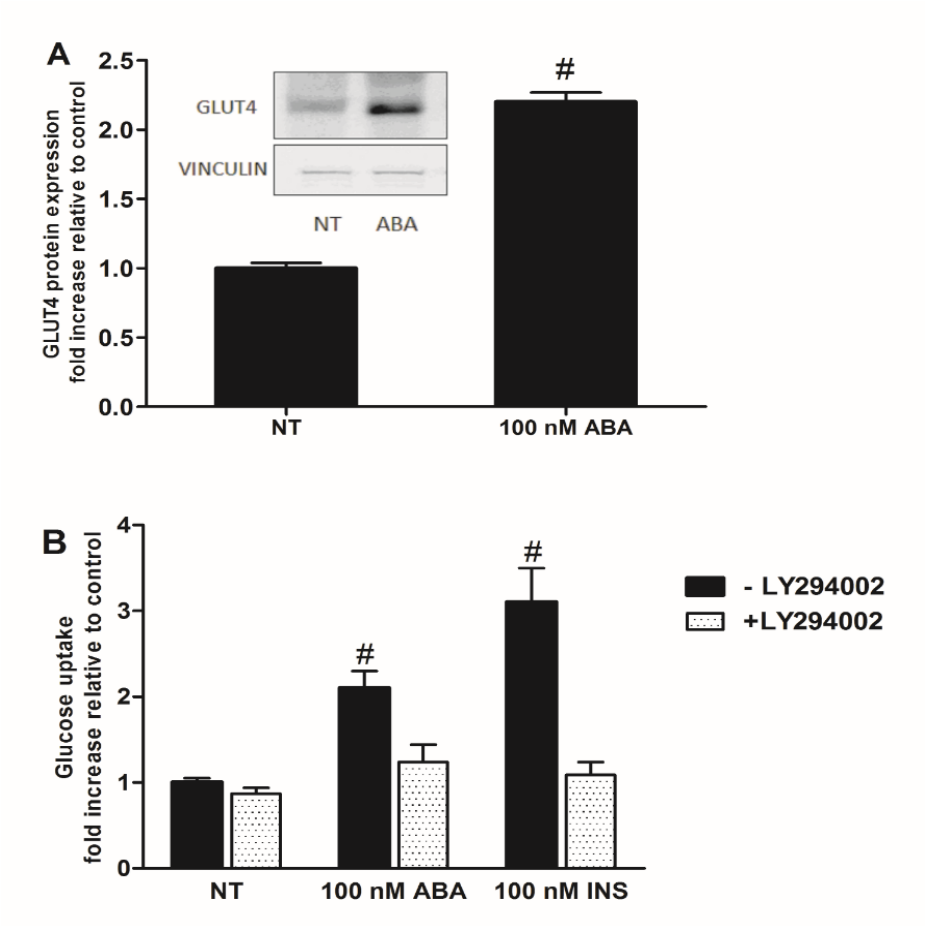

Fig. 16. ABA stimulates GLUT4 expression and function in murine adipocytes via a PI3K-dependent pathway.

A, Western Blot analysis of GLUT4 in 3T3L1 cells differentiated for 5 days in the presence or absence (NT) of 100 nM ABA. Data are mean ± SD of four different experiments. The inset shows a representative Western blot. #p<0.01 ABA relative to NT. **B**, glucose uptake, as measured by the use of [^{14}C]-2-deoxy-D-glucose, in adipocytes incubated in the absence (NT) or in the presence of 100 nM ABA or insulin, without (black columns) or with (dotted columns) the PI3K-specific inhibitor LY294002. Data are mean ± SD of three different experiments. #p<0.01 INS relative to ABA and ABA relative to NT.

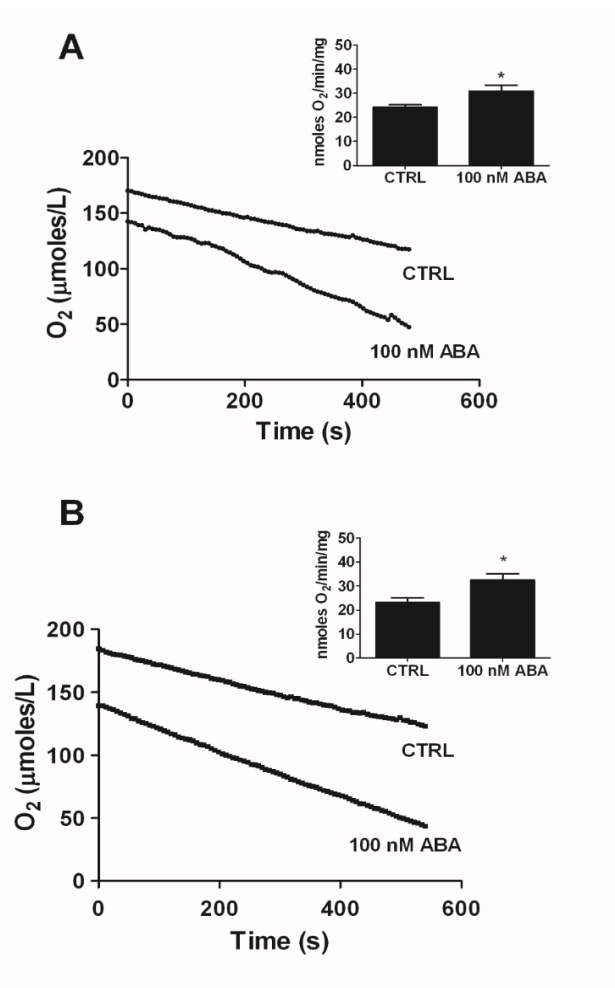

Fig. 17. ABA increases O_2 consumption in 3T3-L1 adipocytes.

3T3-L1 cells were differentiated for 7 days with the differentiation cocktail, in the absence (CTRL) or presence of 100 nM ABA (A), or cells were differentiated for 7 days and then incubated in the absence of the differentiation cocktail for 24 h, without (CTRL) or with 100 nM ABA at 37°C (B). Adipocyte oxygen consumption was measured at 37°C with a micro-amperometric electrode as described in the Methods section. Representative traces from each experimental setting are shown. Each inset shows the mean O_2 consumption from four different experiments, normalized on protein content. *$p<0.05$

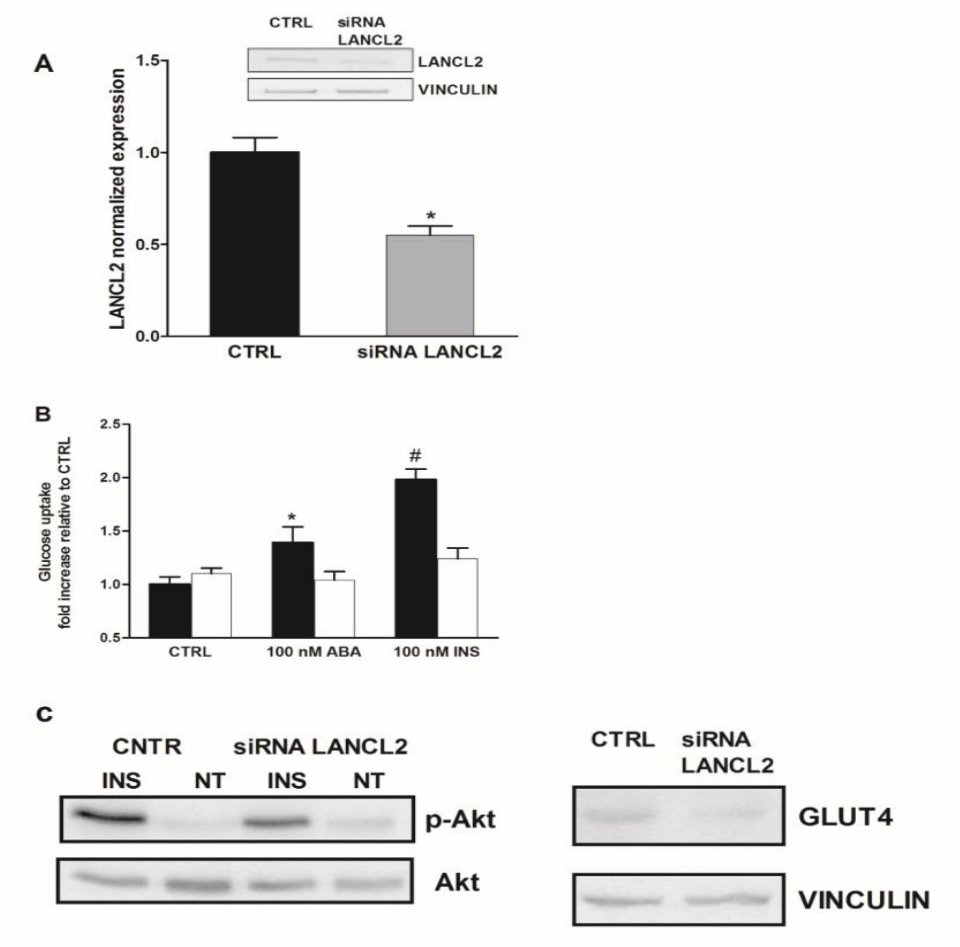

Fig. 18. siRNA-mediated downregulation of LANCL2 expression abrogates the ABA- or insulin-induced glucose uptake in 3T3-L1-derived adipocytes and downregulates Akt phosphorylation after insulin treatment.

3T3-L1-derived adipocytes were transfected with a specific siRNA to downregulate LANCL2 expression (siRNA L2) or with a negative control (CTRL): **A**, Western Blot analysis of cell lysates, revealing downregulation of LANCL2 expression. Inset: a representative experiment. *p<0.05 siRNA LANCL2 relative to CTRL. **B**, glucose uptake, as measured by the use of [^{14}C]-2-deoxy-D-glucose, in CTRL (black columns) or siRNA cells (white columns), incubated (or not) in the presence of 100 nM ABA or insulin. *p<0.05 ABA relative to CTRL #p<0.01 INS relative to ABA. Data are mean ± SD of at least n=3 different experiments.**C,** Western Blot analysis of pAkt and GLUT4 in terminally differentiated 3T3-L1 derived adipocytes, silenced for LANCL2 expression and incubated with 100 nM insulin for 30 min.

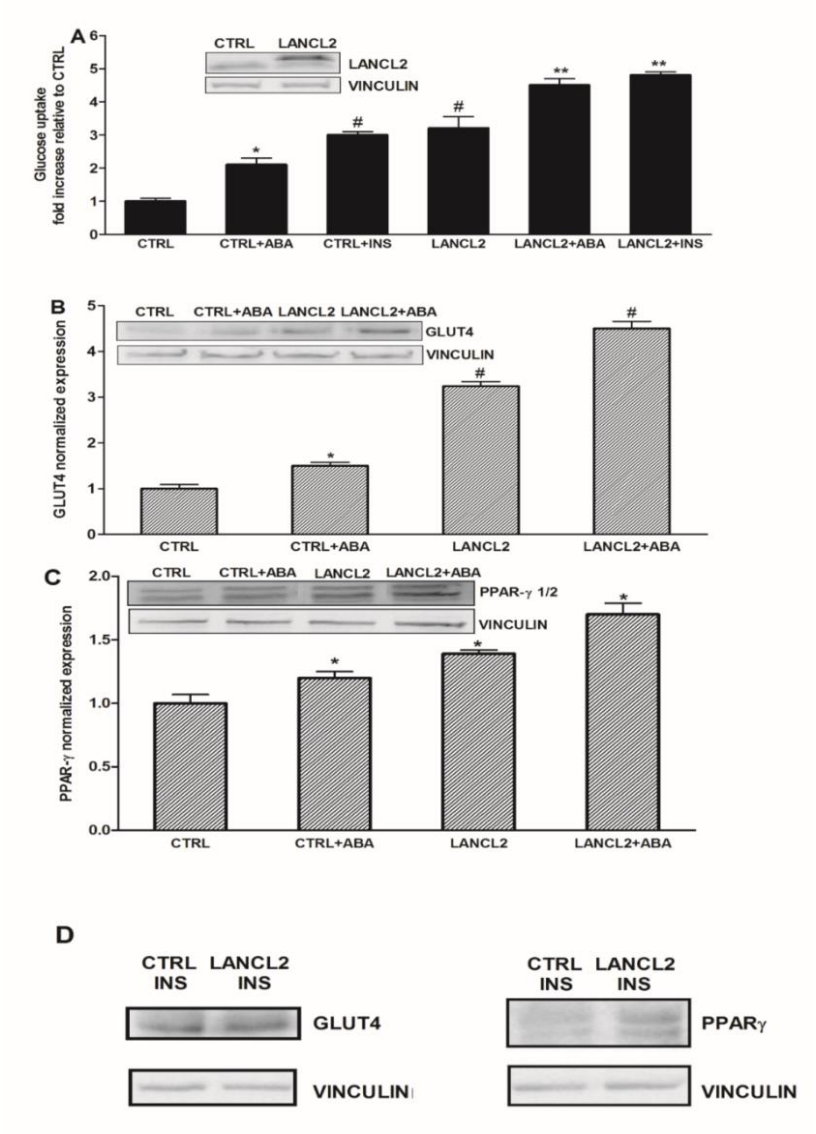

Fig. 19. LANCL2 overexpression stimulates glucose uptake and expression of GLUT4 and PPARγ in 3T3-L1-derived adipocytes.

3T3L1-derived adipocytes were transfected with an empty plasmid (CTRL) or with a LANCL2 plasmid (LANCL2). At 48 h post-transfection, the following assays were performed: **A**, Uptake of [^{14}C]-2-deoxy-D-glucose was measured in CTRL and in LANCL2 cells, incubated for 20 min at 37°C without or with 100 nM ABA or insulin. Inset: a representative Western blot analysis of LANCL2 in lysates from CTRL or LANCL2-transfected cells, showing the

overexpressed, V5-tagged, LANCL2 with a slightly higher molecular mass compared with the native protein. *p<0.05 CTRL+ABA relative to CTRL, #p<0.01 CTRL+INS relative to CTRL+ABA or to CTRL and LANCL2 relative to CTRL, **p<0.01 LANCL2+ABA and LANCL2+INS relative to LANCL2.**B**, **C**, Western Blot (inset) and qPCR analysis of GLUT4 (B) and PPARγ 1/2 (C) in CTRL or LANCL2-transfected cells, incubated for 24 h without or with 100 nM ABA. (B) *p<0.05 CTRL+ABA relative to CTRL, #p<0.01 LANCL2 relative to CTRL and LANCL2+ABA relative to CTRL+ABA; (C) *p<0.05 CTRL+ABA relative to CTRL, LANCL2 relative to CTRL and LANCL2+ABA relative to CTRL+ABA. Data are mean ± SD of at least three different experiments. **D**, Western Blot analysis of GLUT4 and PPARγ 1/2 in CTRL or LANCL2-transfected cells, incubated for 24 h with 100 nM insulin.

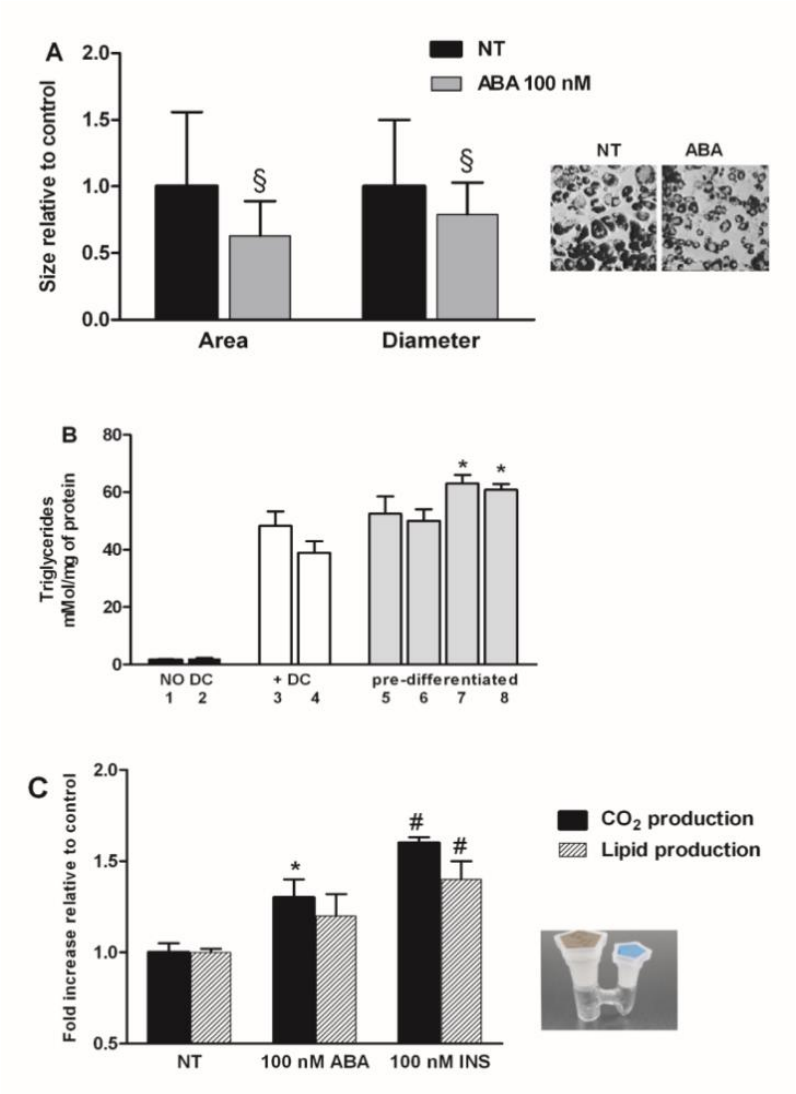

Fig. 20. Effect of ABA on adipocyte size and triglycerides, CO_2 and glucose-derived lipid production.

A, 3T3-L1 pre-adipocytes were cultured for 10 days with an insulin, dexametasone and IBMX-containing differentiating cocktail, without (NT) or with 100 nM ABA. Lipids accumulated were stained with Oil Red O. Right panel: a representative light microscopy phase contrast image. Area and diameter of adipocytes were measured with Image J (≥150 cells for each condition), § $p < 0.005$ relative to NT.**B**, Triglycerides accumulated in 3T3-L1 cells were measured with an enzymatic assay in the following experimental settings: cells cultured for 10 days in complete medium, without the differentiating cocktail (no DC, black

bars), without (bar 1) or with (bar 2) 10 µM ABA; cells cultured for 10 days in the differentiating cocktail (+ DC, white bars), without (bar 3) or with 100 nM ABA (bar 4); cells cultured for 10 days in the differentiating cocktail, then washed and cultured for further 24 h in complete medium (pre-differentiated, grey bars), without (bar 5), or with 100 nM ABA (bar 6) or insulin (bar 7), or ABA and insulin together (bar 8), each at 100 nM. *p<0.05, INS relative to ABA.

C, Production of [^{14}C]-CO_2 (black bars) was measured on 3T3-L1 differentiated for 10 days with the differentiating cocktail, then cultured for 7 h with [U^{14}C]-glucose in a customized glass vial (right panel), in the absence (NT) or in the presence of 100 nM ABA or insulin (INS) (black bars). Synthesis of [^{14}C]-fatty acids (striped bars) was measured on cells differentiated for 6 days, then for further 4 days in the presence of [U^{14}C]-glucose, without (NT) or with 100 nM ABA or insulin (INS). *p<0.05 ABA relative to NT; #p<0.01 INS relative to ABA. All data are the mean ± SD of at least four different experiments.

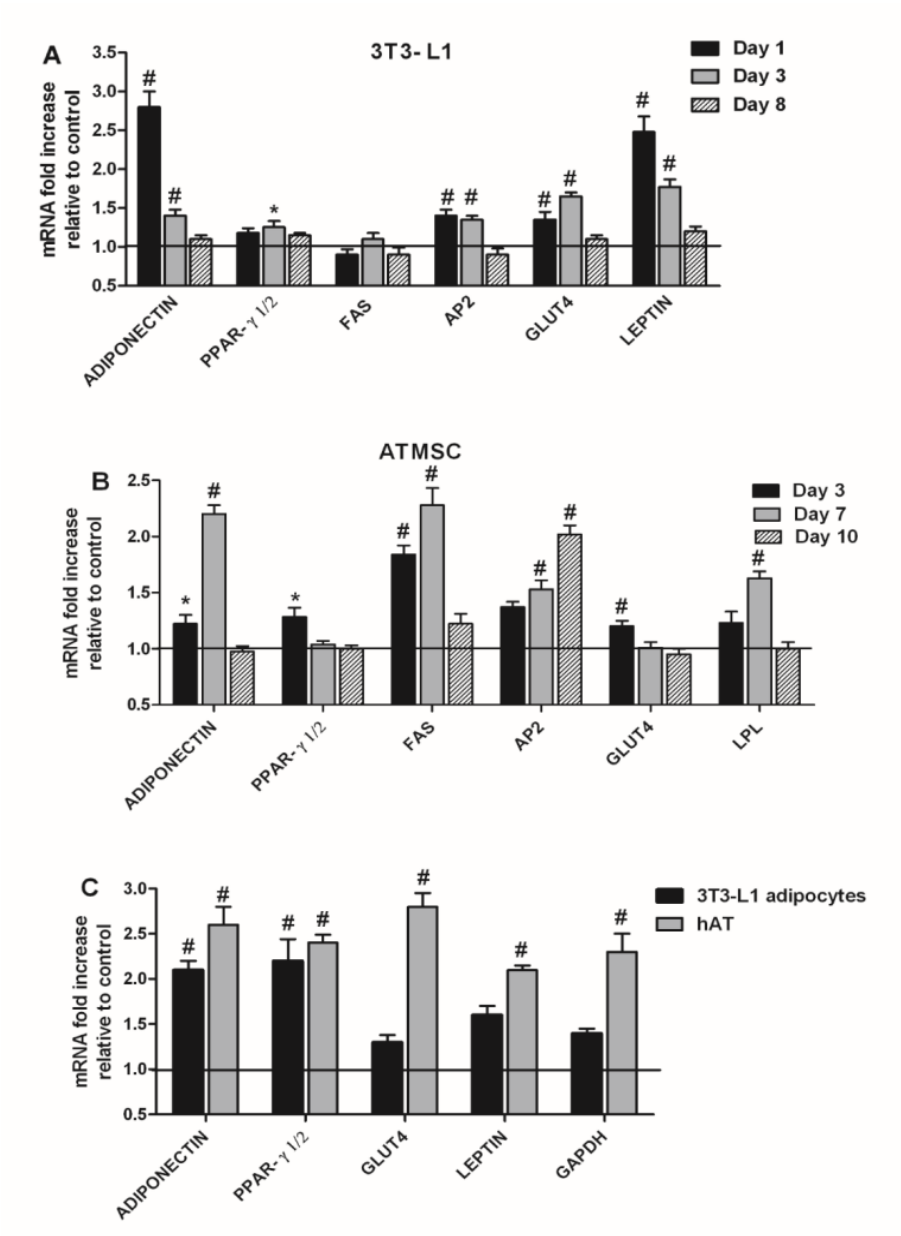

Fig. 21. Transcriptional effects of ABA on adipocytes.

3T3-L1 cells (**A**), or ATMSC (**B**) were differentiated to adipocytes in the absence (control) or presence of 100 nM ABA: at the indicated time points, the mRNA levels of the indicated genes were evaluated by qPCR. Results shown are the mean ± SD from at least four experiments. **C,** 3T3-L1-derived adipocytes, differentiated in the absence of ABA, or human AT biopsies were incubated without (control) or with 100 nM ABA for 4 h. The mRNA levels

of the indicated genes were evaluated by qPCR. Data are mean ± SD of at least four different experiments. #p<0.01 and *p<0.05 ABA, relative to control.

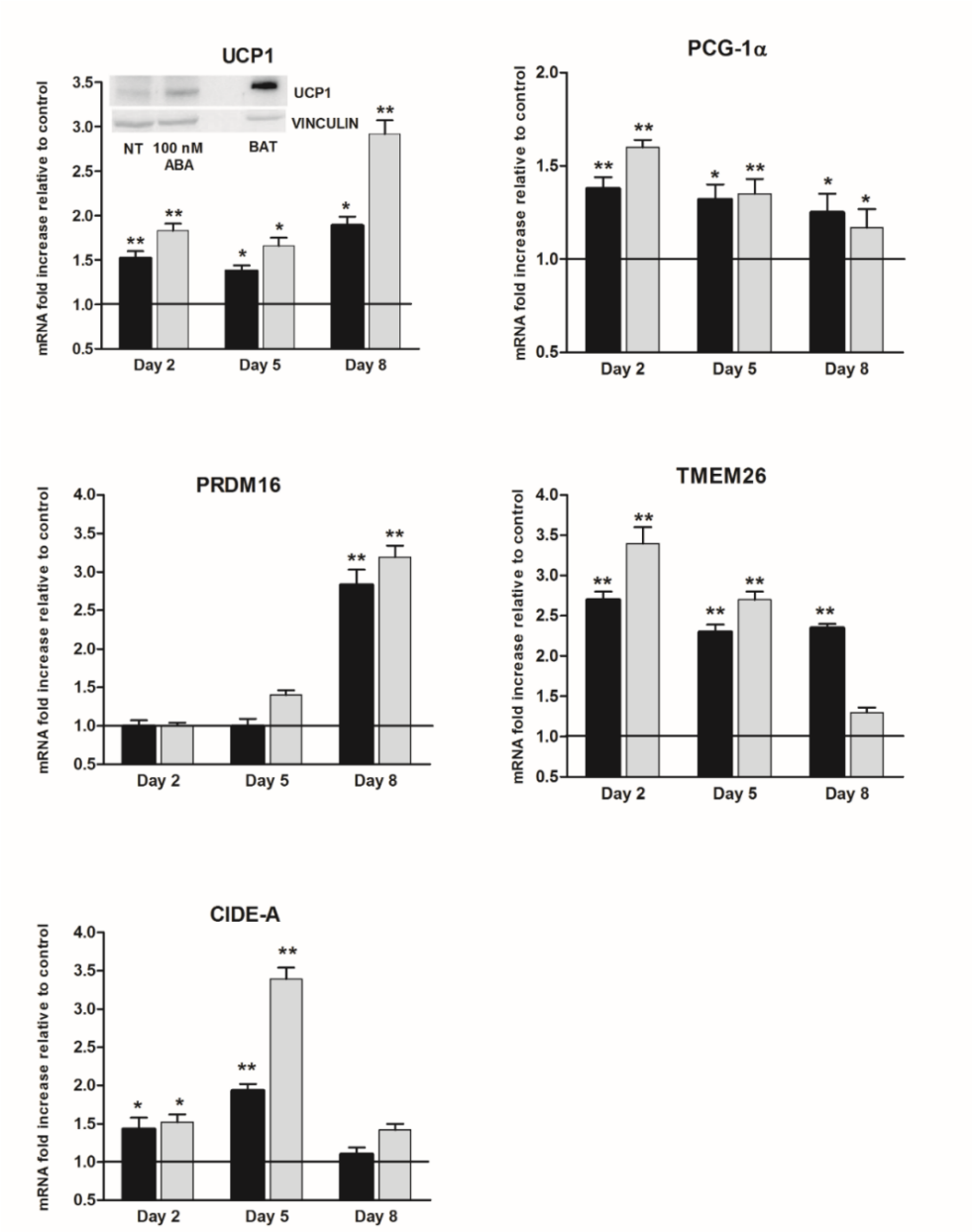

Fig. 22. Browning effect of ABA on 3T3-L1-derived adipocytes. 3T3-L1-derived adipocytes were treated during differentiation without (control) or with 100 nM (black bars) or 10 μM (grey bars) ABA. The expression levels of the indicated genes were measured by qPCR. Data are mean ± SD of at least n=3 different experiments. The inset shows a representative Western blot of UCP1 in 100 μg lysate of 3T3-L1 cells differentiated without (NT) or with ABA. For comparison, the Western blot of UCP1 in 10 μg lysate of murine BAT is shown in the right line. *p<0.05 **p<0.01 ABA relative to control.

REFERENCES

- Abel ED, Peroni O, Kim JK, Kim Y, Boss O, Hadro E, Minnemann T, Shulman GI, Kahn BB. (2001). Adipose-selective targeting of the GLUT4 gene impairs insulin action in muscle and liver. *Nature*; 409: 729-733.
- Allison W.S., Kaplan NO. (1964). The comparative enzymology of triosephosphate dehydrogenase. *J. Biol. Chem*; 239: 2140-2152.
- Ameri P, Bruzzone S, Mannino E, Sociali G, Andraghetti G, Salis A, Ponta ML, Briatore L, Adami GF, Ferraiolo A, Venturini PL, Maggi D, Cordera R, Murialdo G, Zocchi E. (2015). Impaired increase of plasma abscisic acid in response to oral glucose load in type 2 diabetes and in gestational diabetes. *PLoS One*; 10: e0115992.
- Ariemma F, D'Esposito V, Liguoro D, Oriente F, Cabaro S, Liotti A, Cimmino I, Longo M, Beguinot F, Formisano P, Valentino R. (2016). Low-Dose Bisphenol-A Impairs Adipogenesis and Generates Dysfunctional 3T3-L1 Adipocytes. *PLoS One*; 11:e0150762.
- Armoni M, Kritz N, Harel C, Bar-Yoseph F, Chen H, Quon M J, Karnieli E. (2003). Peroxisome Proliferator-activated Receptor-γ represses GLUT4 promoter activity in primary adipocytes, and rosiglitazone alleviates this effect. *Biol. Chem*; 278 :30614–30623.
- Arner P. (2003). The adipocyte in insulin resistance: key molecules and the impact of the thiazolidinediones. *Trends Endocrinol. Metab*; 14 :137–145.
- Baggio LL, Drucker DJ. (2007). Biology of incretins: GLP-1 and GIP. *Gastroenterology ;* 132:2131–2157

- Barbera MJ, Schluter A, Pedraza N, Iglesias R, Villarroya F, Giralt M. (2001). Peroxisome proliferator-activated receptor alpha activates transcription of the brown fat uncoupling protein-1 gene. A link between regulation of the thermogenic and lipid oxidation pathways in the brown fat cell. *J. Biol. Chem*;276 :1486-1493.
- Barneda D, Frontini A, Cinti S, Christian M. (2013). Dynamic changes in lipid droplet-associated proteins in the "browning" of white adipose tissues. *Biochim Biophys Acta*; 1831: 924-933.
- Bassaganya-Riera J, Guri AJ, Lu P, Climent M, Carbo A, Sobral BW, Horne WT, Lewis SN, Bevan DR, Hontecillas R. (2011). Abscisic acid regulates inflammation via ligand-binding domain-independent activation of peroxisome proliferator-activated receptor gamma. *J Biol Chem*; 286:2504-16.
- Bodrato N, Franco L, Fresia C, Guida L, Usai C, Salis A, Moreschi I, Ferraris C, Verderio C, Basile G, Bruzzone S, Scarfì S, De Flora A, Zocchi E. (2009). Abscisic acid activates the murine microglial cell line N9 through the second messenger cyclic ADP-ribose. *J Biol Chem*.; 284:14777-87.
- Bradford MM. (1976). A rapid and sensitive method for the quantitation of microgram quantities of protein utilizing the principle of protein-dye binding. *Anal Biochem*; 72:248-54.
- Brighton CA, Rievaj J, Kuhre RE, Glass LL, Schoonjans K, Holst JJ, Gribble FM, Reimann F. (2015). Bile Acids Trigger GLP-1 Release Predominantly by Accessing Basolaterally Located G Protein–Coupled Bile Acid Receptors. *Endocrinology*. 156: 3961–3970
- Brun RP, Spiegelman BM. (1997) PPARγ and the molecular control of adipogenesis. *J. Endocrinol* ;155: 217–218.

- Bruzzone S, Moreschi I, Usai C, Guida L, Damonte G, Salis A, Scarfì S, Millo E, De Flora A, Zocchi E. (2007). Abscisic acid is an endogenous cytokine in human granulocytes with cyclic ADP-ribose as second messenger. *Proc Natl Acad Sci U S A*.; 104:5759-64.
- Bruzzone S, Bodrato N, Usai C, Guida L, Moreschi I, Nano R, Antonioli B, Fruscione F, Magnone M, Scarfì S, De Flora A, Zocchi E. (2008). Abscisic acid is an endogenous stimulator of insulin release from human pancreatic islets with cyclic ADP ribose as second messenger. *J Biol Chem*.; 283:32188-97.
- Bruzzone S, Ameri P, Briatore L, Mannino E, Basile G, Andraghetti G, Grozio A, Magnone M, Guida L, Scarfì S, Salis A, Damonte G, Sturla L, Nencioni A, Fenoglio D, Fiory F, Miele C, Beguinot F, Ruvolo V, Bormioli M, Colombo G, Maggi D, Murialdo G, Cordera R, De Flora A, Zocchi E. (2012 a.). The plant hormone abscisic acid increases in human plasma after hyperglycemia and stimulates glucose consumption by adipocytes and myoblasts. *FASEB J*.; 26:1251–60.
- Bruzzone S, Basile G, Mannino E, Sturla L, Magnone M, Grozio A, Salis A, Fresia C, Vigliarolo T, Guida L, De Flora A, Tossi V, Cassia R, Lamattina L, Zocchi E. (2012 b.). Autocrine abscisic acid mediates the UV-B-induced inflammatory response in human granulocytes and keratinocytes. J Cell Physiol.; 227:2502-10.
- Cabrera O, Berman DM, Kenyon NS, Ricordi C, Berggren PO, Caicedo A. (2006). The unique cytoarchitecture of human pancreatic islets has implications for islet cell function. *Proc Natl Acad Sci U S A*.; 103: 2334-9.
- Carvalho E, Kotani K, Peroni OD, Kahn BB. (2005). Adipose-specific overexpression of GLUT4 reverses insulin resistance and diabetes in mice

lacking GLUT4 selectively in muscle. *Am. J. Physiol. Endocrinol. Metab*.; 289: E551-E561.

- Centers for Disease Control and Prevention (CDC). (2004). Prevalence of overweight and obesity among adults with diagnosed diabetes--United States, 1988-1994 and 1999-2002. *MMWR Morb Mortal Wkly Rep*.; 53:1066-8.
- Chamnan P, Simmons RK, Forouhi NG, Luben RN, Khaw KT, Wareham NJ, Griffin SJ. (2011). Incidence of type 2 diabetes using proposed HbA1c diagnostic criteria in the european prospective investigation of cancer-norfolk cohort: implications for preventive strategies. *Diabetes Care*; 34:950-6
- Christensen LW, Kuhre RE, Janus C, Svendsen B, Holst JJ. (2015). Vascular, but not luminal, activation of FFAR1 (GPR40) stimulates GLP-1 secretion from isolated perfused rat small intestine. *Physiol Rep*.; 3(9). pii: e12551
- Deacon CF, Plamboeck A, Rosenkilde MM, de Heer J, Holst JJ. (2006). GIP-(3–42) does not antagonize insulinotropic effects of GIP at physiological concentrations. *Am. J. Physiol. Endocrinol. Metab*.; 291: E468–E475.
- de Souza CJ, Eckhardt M, Gagen K, Dong M, Chen W, Laurent D, Burkey BF. (2001). Effects of pioglitazone on adipose tissue remodeling within the setting of obesity and insulin resistance. *Diabetes*; 50:1863–1871.
- Desvergne B, Wahli W. (1999). Peroxisome proliferator-activated receptors: nuclear control of metabolism. *Endocr. Rev*., 20: 649– 688.
- Ezcurra M, Reimann F, Gribble FM, Emery E. (2013). Molecular mechanisms of incretin hormone secretion. *Curr Opin Pharmacol*.;13: 922-927.
- Farmer SR. (2006). Transcriptional control of adipocyte formation. *Cell Metab*.; 4:263–273.
- Favaretto F, Milan G, Collin GB, Marshall JD, Stasi F, Maffei P, Vettor R, Naggert JK. (2014). GLUT4defects in adiposetissue are earlysigns of

metabolicalterations in Alms1GT/GT, a mousemodel for obesity and insulinresistance. *PLoS One*; 9:e109540.

- Forest T, Holder D, Smith A, Cunningham C, Yao X, Dey M, Frederick C, Prahalada S. (2014). Characterization of the exocrine pancreas in the male Zucker diabetic fatty rat model of type 2 diabetes mellitus following 3 months of treatment with sitagliptin. *Endocrinology*; 155: 783-792.
- Fresia C, Vigliarolo T, Guida L, Booz V, Bruzzone S, Sturla L, Di Bona M, Pesce M ,Usai C, De Flora A, Zocchi E (2016). G-protein coupling and nuclear translocation of the human abscisic acid receptor LANCL2. *Sci Rep*; 6:26658.
- Garry PS, Ezra M, Rowland MJ, Westbrook J, Pattinson KT. (2015) The role of the nitric oxide pathway in brain injury and its treatment--from bench to bedside. Exp Neurol.; .263:235-43.
- Gesta S, Tseng YH, Kahn CR. (2007). Developmental origin of fat: tracking obesity to its source. *Cell*; 131:242–256.
- Gromada J., Franklin I, Wollheim CB. (2007). Alpha-cells of the endocrine pancreas: 35 years of research but the enigma remains. *Endocr Rev*.;28: 84-116.
- Guri AJ, Hontecillas R, Si H, Liu D, Bassaganya-Riera J. (2007). Dietary abscisic acid ameliorates glucose tolerance and obesity-related inflammation in db/db mice fed high-fat diets. *Clin. Nutr. Edinb. Scotl*.;26:107–116.
- Guri AJ, Hontecillas R, Ferrer G, Casagran O, Wankhade U, Noble AM, Eizirik DL, Ortis F, Cnop M, Liu D, Si H, Bassaganya-Riera J.(2008). Loss of PPAR gamma in immune cells impairs the ability of abscisic acid to improve insulin sensitivity by suppressing monocyte chemoattractant protein-1 expression and macrophage infiltration into white adipose tissue. *J Nutr Biochem*.; 19:216–28.
- Guri AJ, Misyak SA, Hontecillas R, Hasty A, Liu D, Si H, Bassaganya-Riera J.

(2010 a.). Abscisic acid ameliorates atherosclerosis by suppressing macrophage and CD4+ T cell recruitment into the aortic wall. *J Nutr Biochem*.; 21: 1178-1185.

- Guri AJ, Hontecillas R, Bassaganya-Riera J. (2010 b.). Abscisic acid synergizes with rosiglitazone to improve glucose tolerance and down-modulate macrophage accumulation in adipose tissue: possible action of the cAMP/PKA/PPAR γ axis. *Clin Nutr*.; 29: 646-653.
- Hirasawa A, Tsumaya K, Awaji T, Katsuma S, Adachi T, Yamada M, Sugimoto Y, Miyazaki S, Tsujimoto G. (2005). Free fatty acids regulate gut incretin glucagon-like peptide-1 secretion through GPR120. *Nat Med*; 11:90-4.
- Holst JJ, Deacon CF, Vilsbøll T, Krarup T, Madsbad S. (2008). Glucagon-like peptide-1, glucose homeostasis and diabetes. *Trends Mol Med*.; 14:161-8.
- Holst JJ, Seino Y. (2009). GLP-1 receptor agonists: targeting both hyperglycaemia and disease processes in diabetes. *Diabetes Res Clin Pract.*; 85:1-3.
- Holst JJ, Christensen M, Lund A, de Heer J, Svendsen B, Kielgast U, Knop FK. (2011). Regulation of glucagon secretion by incretins. *Diabetes Obes Metab*.; 13 Suppl 1:89-94.
- Huang S, Czech MP. (2007). The GLUT4 Glucose Transporter. Cell Metab.;5:237-252
- Hui X, Gu P, Zhang X, Nie T, Pan, Y.Wu, D. Feng T, Zhong C, Wang Y, Lam KS, Xu A. (2015). Adiponectin Enhances Cold-Induced Browning of Subcutaneous Adipose Tissue via Promoting M2 Macrophage Proliferation. *Cell Metab*.; 22: 279-290.
- Jang HJ, Kokrashvili Z, Theodorakis MJ, Carlson OD, Kim BJ, Zhou J, Kim HH, Xu X, Chan SL, Juhaszova M, Bernier M, Mosinger B, Margolskee RF, Egan JM.

(2007) Gut-expressed gustducin and taste receptors regulate secretion of glucagon-like peptide-1. *Proc Natl Acad Sci USA*.;104: 15069-15074.

- Katona I, Weis J. (2017). Diseases of the peripheral nerves. Handb Clin Neurol.; 145:453-474.
- Keira SM, Ferreira LM, Gragnani A, Duarte IS, Campaner AB, Durão MS. (2004). Experimental model for establishment of hypoxia in 75 cm2 culture flasks. Acta Cir Bras, Vol 19.
- Kershaw EE, Flier JS. (2004). Adipose tissue as an endocrine organ. *J Clin Endocrinol Metab*.; 89:2548-56.
- Kielgast U, Holst JJ, Madsbad S. (2009). Treatment of type 1 diabetic patients with glucagonlike peptide-1 (GLP-1) and GLP-1R agonists. *Curr Diabetes Rev*. 5:266-75.
- Klingler JP, Batelli G, Zhu JK. (2010). ABA receptors: the START of a new paradigm in phytohormone signalling. *J Exp Bot*.; 61:3199-210.
- Knop FK, Vilsboll T, Holst JJ. (2009). Incretin-based therapy of type 2 diabetes mellitus. Curr Protein Pept Sci. 2009. 10: 46-55.
- Koerner A, Kratzsch J, Kiess W. (2005). Adipocytokines: leptin--the classical, resistin--the controversical, adiponectin--the promising, and more to come. *Best Pract. Res. Clin. Endocrinol. Metab*.; 19:525-546.
- Kuhre RE, Frost CR, Svendsen B, Holst JJ. (2014). Molecular mechanisms of glucose-stimulated GLP-1 secretion from perfused rat small intestine. *Diabetes*;64: 370–382.
- Landlinger C, Salzer U, Prohaska R. (2006). Myristoylation of human LanC-like protein 2 (LANCL2) is essential for the interaction with the plasma membrane and the increase in cellular sensitivity to adriamycin. *Biochim Biophys Acta*.; 1758:1759-67.

- Lee YH, Jung YS, Choi D. (2014). Recent advance in brown adipose physiology and its therapeutic potential. *Exp. & Mol. Med*.;46: e78.
- Le Page-Degivry MT, Bidard JN, Rouvier E, Bulard C, Lazdunski M. (1986). Presence of abscisic acid, a phytohormone, in the mammalian brain. *Le Proc Natl Acad Sci U S A*.; 83:1155-8.
- Liu XW, Zi Y, Liu YE, Zhang YB, Xiang LB, Hou MX. (2015). Melatonin exerts protective effect on N2a cells under hypoxia conditions through Zip1/ERK pathway. Neurosci Lett.;595:74-80.
- Livak KJ, Schmittgen TD. (2001). Analysis of relative gene expression data using real-time quantitative PCR and the $^{2-\Delta\Delta}$ Ct method*. Methods*. 25:402-408.
- Lu P, Hontecillas R, Philipson CW, Bassaganya-Riera J. (2014). Lanthionine synthetase component C-like protein 2: a new drug target for inflammatory diseases and diabetes. *Curr Drug Targets*.;15: 565-572.
- Maeda K. (2007). Role of adiponectin and adipocyte fatty acid binding protein in the metabolic syndrome. *Diabetes. Res. Clin. Pract*.; 77 Suppl 1: S17-22.
- Magnone M, Bruzzone S, Guida L, Damonte G, Millo E, Scarfi S, Usai C, Sturla L, Palombo D, De Flora A, Zocchi E. (2009). Abscisic acid released by human monocytes activates monocytes and vascular smooth muscle cell responses involved in atherogenesis*. J Biol Chem*.; 284:17808-18.
- Magnone M, Ameri P, Salis A, Andraghetti G, Emionite L, Murialdo G, De Flora A, Zocchi E. (2015). Microgram amounts of abscisic acid in fruit extracts improve glucose tolerance and reduce insulinemia in rats and in humans. *FASEB J*.; 29:4783–4793.
- Marini C, Salani B, Massollo M, Amaro A, Esposito AI, Orengo AM, Capitanio S, Emionite L, Riondato M, Bottoni G, Massara C, Boccardo S, Fabbi M, Campi C, Ravera S, Angelini G, Morbelli S, Cilli M, Cordera R, Truini M, Maggi D, Pfeffer

U, Sambuceti G. (2013). Direct inhibition of hexokinase activity by metformin at least partially impairs glucose metabolism and tumor growth in experimental breast cancer. *Cell Cycle*; 12:3490-3499.

- Michael LF, Wu Z, Cheatham RB, Puigserver P, Adelmant G, Lehman JJ, Kelly DP, Spiegelman BM. (2001). Restoration of insulin-sensitive glucose transporter (GLUT4) gene expression in muscle cells by the transcriptional coactivator PGC-1. *Proc. Natl. Acad. Sci USA*; 98:3820–3825.
- Misko TP, Schilling RJ, Salvemini D, Moore WM, Currie MG. (1993). A fluorometric assay for the measurement of nitrite in biological samples. Anal Biochem.; 214:11-6.
- Moncada S, Higgs EA. (1991). Endogenous nitric oxide: physiology, pathology and clinical relevance. Eur J Clin Invest.; 21:361-74.
- Moreschi I, Bruzzone S, Nicholas RA, Fruscione F, Sturla L, Benvenuto F, Usai C, Meis S, Kassack MU, Zocchi E, De Flora A. (2006). Extracellular NAD+ is an agonist of the human P2Y11 purinergic receptor in human granulocytes. *J Biol Chem*.;281: 31419-31429.
- Nauck MA, Kleine N, Orskov C, Holst JJ, Willms B, Creutzfeldt W. (1993). Normalization of fasting hyperglycaemia by exogenous glucagon-like peptide 1 (7-36 amide) in type 2 (non-insulin-dependent) diabetic patients. *Diabetologia*; 36:741–744.
- Okuno A, Tamemoto H, Tobe K, Ueki K, Mori Y, Iwamoto K, Umesono K, Akanuma Y, Fujiwara T, Horikoshi H, Yazaki Y, Kadowaki T. (1998). Troglitazone increases the number of small adipocytes without the change of white adipose tissue mass in obese *Zucker rats. Clin. Invest*.; 101: 1354-1361.
- Olokoba Abdulfatai B, Obateru Olusegun A, Olokoba Lateefat B. (2012). Type 2 diabetes mellitus: a review of current trends. *Oman Med J*.; 27:269-73.

- Qi CC, Zhang Z, Fang H, Liu J, Zhou N, Ge JF, Chen FH, Xiang CB, Zhou JN. (2014). Antidepressant effects of abscisic acid mediated by the downregulation of corticotrophin-releasing hormone gene expression in rats. Int J Neuropsychopharmacol.;18(4). pii: pyu006.
- Reimann F, Williams L, da Silva Xavier G, Rutter GA, Gribble FM. (2004). Glutamine potently stimulates glucagon-like peptide-1 secretion from GLUTag cells. *Diabetologia* ; 47: 1592–1601.
- Reimer RA, Darimont C, Gremlich S, Nicolas-Métral V, Rüegg UT, Macé K. (2001). A human cellular model for studying the regulation of glucagon-like peptide-1 secretion. *Endocrinology* ; 142:4522-8.
- Riederer P, Korczyn AD, Ali SS, Bajenaru O, Choi MS, Chopp M, Dermanovic-Dobrota V, Grünblatt E, Jellinger KA, Kamal MA, Kamal W, Leszek J, Sheldrick-Michel TM, Mushtaq G, Meglic B, Natovich R, Pirtosek Z, Rakusa M, Salkovic-Petrisic M, Schmidt R, Schmitt A, Sridhar GR, Vécsei L, Wojszel ZB, Yaman H, Zhang ZG, Cukierman-Yaffe T. (2017). The diabetic brain and cognition. *J Neural Transm.*; doi: 10.1007/s00702-017-1763-2.
- Rosen ED, Sarraf P, Troy AE, Bradwin G, Moore K, Milstone DS, Spiegelman BM, Mortensen RM. (1999). PPAR gamma is required for the differentiation of adipose tissue in vivo and in vitro. *Mol. Cell*; 4:611–617.
- Rosen ED, Spiegelman BM. (2006). Adipocytes as regulators of energy balance and glucose homeostasis. *Nature*; 444:847-53.
- Saha JK, Xia J, Grondin JM, Engle SK, Jakubowski JA. (2005). Acute hyperglycemia induced by ketamine/xylazine anesthesia in rats: mechanisms and implications for preclinical models. *Exp Biol Med*.; 230: 777-784.
- Sakurai H, DobbsR, Unger RH. (1974). Somatostatin-induced changes in insulin and glucagon secretion in normal and diabetic dogs. *J Clin Invest*; 54:1395-402.

- Saltiel AR, Olefsky JM. (1996). Thiazolidinediones in the treatment of insulin resistance and type II diabetes. *Diabetes*; 45:1661–1669.
- Saltiel AR, Kahn CR. (2001). Insulin signalling and the regulation of glucose and lipid metabolism. *Nature*; 414:799-806.
- Samols E, Bonner-Weir S, Weir GC. (1986). Intra-islet insulin-glucagon-somatostatin relationships. *Clin Endocrinol Metab*.;15: 33-58.
- Sandoval DA, D'Alessio DA. (2015). Physiology of Proglucagon Peptides: Role of Glucagon and GLP-1 in Health and Disease. *Physiol Rev*.; 95:513-548.
- Sánchez-Sarasúa S, Moustafa S, García-Avilés Á, López-Climent MF, Gómez-Cadenas A, Olucha-Bordonau FE, Sánchez-Pérez AM. (2016). The effect of abscisic acid chronic treatment on neuroinflammatory markers and memory in a rat model of high-fat diet induced neuroinflammation. Nutr Metab.; 13:73
- Scarfi S, Ferraris C, Fruscione F, Fresia C, Guida L, Bruzzone S, Usai C, Parodi A, Millo E, Salis A, Burastero G, De Flora A, Zocchi E. (2008). Cyclic ADP-ribose-mediated expansion and stimulation of human mesenchymal stem cells by the plant hormone abscisic acid. *Stem Cells*; 26:2855–2864.
- Scarfì S, Fresia C, Ferraris C, Bruzzone S, Fruscione F, Usai C, Benvenuto F, Magnone M, Podestà M, Sturla L, Guida L, Albanesi E, Damonte G, Salis A, De Flora A, Zocchi E. (2009). The plant hormone abscisic acid stimulates the proliferation of human hemopoietic progenitors through the second messenger cyclic ADP-ribose. *Stem Cells*; 27:2469-77.
- Simão F, Pagnussat AS, Seo JH, Navaratna D, Leung W, Lok J, Guo S, Waeber C, Salbego CG, Lo EH. (2012). Pro-angiogenic effects of resveratrol in brain endothelial cells: nitric oxide-mediated regulation of vascular endothelial growth factor and metalloproteinases. J Cereb Blood Flow Metab.; 32:884-95.

- Smith RE, Horwitz BA. (1969). Brown fat and thermogenesis. *Physiol Rev*.; 49:330-425
- Smith SA. (2003). Central role of the adipocyte in the insulin-sensitising and cardiovascular risk modifying actions of the thiazolidinediones. *Biochimie*.; 85:1219-1930.
- Sturla L, Fresia C, Guida L, Bruzzone S, Scarfì S, Usai C, Fruscione F, Magnone M, Millo E, Basile G, Grozio A, Jacchetti E, Allegretti M, De Flora A, Zocchi E. (2009). LANCL2 is necessary for abscisic acid binding and signaling in human granulocytes and in rat insulinoma cells*. J Biol Chem*.; 284:28045–57.
- Sturla L, Fresia C, Guida L, Grozio A, Vigliarolo T, Mannino E, Millo E, Bagnasco L, Bruzzone S, De Flora A, Zocchi E. (2011). Binding of abscisic acid to human LANCL2. *Biochem Biophys Res Commun*.; 415:390-5.
- Tiraby C, Tavernier G, Lefort C, Larrouy D, Bouillaud F, Ricquier D, Langin D. (2003). Acquirement of brown fat cell features by human white adipocytes. *J Biol Chem.*; 278:33370-6.
- Toda N, Ayajiki K, Okamura T. (2009). Cerebral blood flow regulation by nitric oxide in neurological disorders. Can J Physiol Pharmacol.; 87:581-94.
- Todd JF, Wilding JP, Edwards CM, Khan FA, Ghatei MA, Bloom SR. (1997). Glucagon-like peptide-1 (GLP-1): a trial of treatment in non-insulin-dependent diabetes mellitus. *Eur J Clin Investig*.; 27: 533–536.
- Tolhurst G, Zheng Y, Parker HE, Habib AM, Reimann F, Gribble FM. (2011). Glutamine triggers and potentiates glucagon-like peptide-1 secretion by raising cytosolic Ca2+ and cAMP. *Endocrinology*;.152: 405-413.
- Tontonoz P, Hu E, Spiegelman BM. (1994). Stimulation of adipogenesis in fibroblasts by PPARγ-2, a lipid-activated transcription factor. *Cell*;.79:1147-1156.

- Tossi V, Cassia R, Bruzzone S, Zocchi E, Lamattina L. (2012). ABA says NO to UV-B: a universal response? *Trends Plant Sci*.; 17:510-517.
- Uldry M, Yang W, St-Pierre J, Lin J, Seale P, Spiegelman BM. (2006). Complementary action of the PGC-1 coactivators in mitochondrial biogenesis and brown fat differentiation. *Cell Metab*.; 3:333–341.
- Vigliarolo T, Guida L, Millo E, Fresia C, Turco E, De Flora A, Zocchi E. (2015). Abscisic Acid transport in Human Erythrocytes. *J Biol Chem*.; 290: 13042-13052.
- Wallberg-Henriksson H, Zierath JR. (2001). GLUT4: a key player regulating glucose homeostasis? Insights from transgenic and knockout mice. *Mol Membr Biol*; 18:205-11.
- Wu J, Boström P, Sparks LM, Ye L, Choi JH, Giang AH, Khandekar M, Virtanen KA, Nuutila P, Schaart G, Huang K, Tu H, van Marken Lichtenbelt WD, Hoeks J, Enerbäck S, Schrauwen P, Spiegelman BM. (2012). Beige adipocytes are a distinct type of thermogenic fat cell in mouse and human. *Cell*; 150:366-76.
- Zeng M, van der Donk WA, Chen J. (2014). Lanthionine synthetase C-like protein 2 (LanCL2) is a novel regulator of Akt. *Mol. Biol. Cell*.; 25:3954-3961.
- Zuk PA, Zhu M, Mizuno H, Huang J, Futrell JW, Katz AJ, Benhaim P, Lorenz HP, Hedrick MH. (2001). Multilineage cells from human adipose tissue: implications for cell-based therapies. *Tissue Eng*.; 7:211-28